



Petroleum Systems of Lebanon : an update and review

R. Ghalayini, F. Nader, S. Bou Daher, N. Hawie, W. Chbat

► To cite this version:

R. Ghalayini, F. Nader, S. Bou Daher, N. Hawie, W. Chbat. Petroleum Systems of Lebanon : an update and review. Journal of Petroleum Geology, 2018, 41 (2), pp.189-214. hal-01940792

HAL Id: hal-01940792

<https://ifp.hal.science/hal-01940792>

Submitted on 30 Nov 2018

HAL is a multi-disciplinary open access archive for the deposit and dissemination of scientific research documents, whether they are published or not. The documents may come from teaching and research institutions in France or abroad, or from public or private research centers.

L'archive ouverte pluridisciplinaire **HAL**, est destinée au dépôt et à la diffusion de documents scientifiques de niveau recherche, publiés ou non, émanant des établissements d'enseignement et de recherche français ou étrangers, des laboratoires publics ou privés.

1
2
3
4
5
6
7
8
9
10
11
12
13
14
15
16
17
18
19
20
21
22
23
24
25
26
27
28
29
30
31
32
33
34
35
36
37
38
39
40
41
42
43
44
45
46
47
48
49
50
51
52
53
54
55
56
57
58
59
60

1 **Title:** Petroleum Systems of Lebanon

2 **Authors:** Ghalayini, R.⁽¹⁾, Nader, F.H. ⁽²⁾, Bou Daher, S. ⁽³⁾, Hawie, N. ⁽⁴⁾ & Chbat,

3 W.E. ⁽¹⁾

4 **Institutions:**

5 ⁽¹⁾Lebanese Petroleum Administration, Georges Akouri Street, Beirut, Lebanon

6 ⁽²⁾ Geology Department, Geosciences Division IFP Energies Nouvelles, 1 & 4 Av.

7 de Bois-Préau, 92852 Rueil-Malmaison, France.

8 ⁽³⁾ Department of Geosciences and Natural Resource Management, University of

9 Copenhagen, Øster Volgade 10, 1350 Copenhagen, Denmark.

10 ⁽⁴⁾ BeicipFranlab, 232 Av. de Bois-Préau, 92502 Rueil-Malmaison, France.

11 **Abstract**

12 Extensive 3D seismic data offshore Lebanon together with new investigations of

13 the onshore domain have resulted in a considerable wealth of information on the

14 regional geology and petroleum prospectivity. This article presents a new

15 interpretation of the Levant margin offshore Lebanon with an up-to-date review

16 of the geology of Lebanon and a new comprehensive insight on the petroleum

17 systems along the Eastern Mediterranean sector. The Lebanese onshore and

18 offshore territories are separated in this study into four different domains: the

19 deep basin, the Lattakia Ridge, the Levant margin and the onshore. Each of these

20 domains is marked by a general structural style and various stratigraphic

21 architectures, resulting in different source-reservoir-trap configurations. The

22 new subdivision impacts exploration as it highlights specific geographic areas

23 having distinct petroleum systems. This study takes into account all previously

24 published geological knowledge and provides new results from stratigraphic,

25 structural and geochemical investigations to propose a summary of the potential
26 petroleum systems for each domain, on the eve of Lebanon first offshore
27 licensing round.

28 Introduction

29 Lebanon, part of the larger Levant region, is located in the NW part of the
30 Arabian plate along its western active boundary with Africa (fig. 1). This area is
31 marked by the passage of the Levant Fracture System (LFS), the fold and thrust
32 belt of the Palmyrides ranges to the east and the stable foreland Levant basin to
33 the west. Lebanon and its offshore are considered as a promising petroleum
34 province as a result of more than 70 tcf of proven natural gas reserves in nearby
35 countries, following the discovery of Tamar, Leviathan, Aphrodites and Zohr
36 between 2006 and 2015 (fig. 2). Onshore, recoverable reserves of Syria are
37 estimated at about 2.5 billion bbl of oil and about 8.5 TCF of gas, with productive
38 fields in the Palmyrides, the Euphrates graben and the Sinjar high (Barrier *et al.*,
39 2014).

40
41 The latest petroleum activities in the Levant and the promising potential of
42 Lebanon have prompted the Lebanese government to acquire an extensive
43 amount of multiclient 3D seismic data to aid exploration offshore. Improved
44 knowledge of the geology of the Levant region was achieved by using this
45 unprecedented wealth of information and seismic data coverage and by
46 attracting considerable academic and industrial research projects, referenced
47 herein. A new model for the stratigraphic setting and filling of the basin has been
48 suggested based on seismic data and extensive fieldwork (Hawie *et al.*, 2015).

1
2
3
4
5
6
7
8
9
10
11
12
13
14
15
16
17
18
19
20
21
22
23
24
25
26
27
28
29
30
31
32
33
34
35
36
37
38
39
40
41
42
43
44
45
46
47
48
49
50
51
52
53
54
55
56
57
58
59
60

49 The structural framework of the Levant basin and margin has been described on
50 the light of new 3D reflection seismic data interpretation, and modelling
51 (Ghalayini *et al.*, 2014; and references therein). A new geochemical assessment
52 of source rock potential based on extensive sampling onshore Lebanon has also
53 been completed (Bou Daher *et al.*, 2014; Bou Daher *et al.*, 2015). This has
54 resulted in the development of a new basin model for Lebanon and its offshore
55 based on an integration of all the newly acquired knowledge, providing an
56 updated picture of the hydrocarbon potential of Lebanon (Bou Daher *et al.*,
57 2016). In addition, a refined model for the crustal structure of the Levant Basin
58 was proposed (Inati *et al.*, 2016), which directly impacts the petroleum systems
59 and the source rock maturity.
60
61 This article summarizes the results of the latest geological and petroleum
62 investigations in Lebanon and adds new up-to-date data – especially with regard
63 to potential petroleum systems. First, it presents new interpretation of the
64 Levant margin offshore Lebanon since the carbonate prospects have attracted
65 major attention following the Zohr discovery in carbonate reservoirs offshore
66 Egypt. Second, it subdivides the region into geological domains based on
67 multitude of stratigraphic, structural and geochemical data. Third, it discusses
68 the various petroleum aspects of each domain (potential source rocks,
69 reservoirs, and traps) and points out new objectives based on recent data and
70 neighboring discoveries. These results serve as a basis for the understanding of
71 the petroleum potential of Lebanon and provide a good case study on
72 exploration effectiveness and strategy at a critical time as the first offshore
73 licensing round has been set.

74 Exploration history

75

76 Petroleum exploration in Lebanon started with the first legal decree issued in
77 1933 and amended in 1936. Twelve companies were actively involved in
78 exploration in Lebanon among which the 'Compagnie Libanaise des Pétroles'
79 (CLP) and the 'Syria Petroleum Company' (SPC) were the largest (Wetzel, 1974).
80 The SPC, which was a subsidiary of the Iraq Petroleum Company, drilled the first
81 well in Terbol in 1947 and failed to reach economic accumulations. It has since
82 relinquished all its concessions in Lebanon and concentrated its activity in Syria.
83 The CLP drilled five wells in the Bekaa between 1953 and 1964, four of which
84 with foreign partners, but without any commercial result. The CLP was the only
85 company to hold concessions amounting to 5200 Km². Exploration was not only
86 undertaken onshore, as Shaheen-Oxoco had offshore permits next to Tripoli. In
87 1970, the first seismic data was acquired by Oxoco offshore north Lebanon and
88 in 1971 Delta acquired 320 km of 2D seismic lines in addition to a gravity survey
89 on the Shaheen permit.

90

91 The acquisition of several regional 2D seismic reflection surveys by Spectrum
92 and TGS in 2000 and 2002 respectively, led to mapping of several promising
93 leads in the subsalt units. Between 2006 and 2012 PGS acquired 9700 Km² of
94 multicient 3D seismic data followed by Spectrum who also acquired additional
95 5172 km² of multicient 3D seismic data between 2012 and 2013 in the deep-
96 water offshore Lebanon resulting in an exceptional wealth of information for the
97 offshore basin. The new data has indicated a promising hydrocarbon potential

1
2
3
4
5
6
7
8
9
10
11
12
13
14
15
16
17
18
19
20
21
22
23
24
25
26
27
28
29
30
31
32
33
34
35
36
37
38
39
40
41
42
43
44
45
46
47
48
49
50
51
52
53
54
55
56
57
58
59
60

98 for Lebanon (Roberts and Peace, 2007) prompting the government to issue new
99 decrees in 2017 to regulate the offshore exploration.

100 **Tectonic and crustal setting**

101

102 The present-day tectonic framework is the result of the complex geodynamic
103 evolution of the region through geologic time. Two large structures are
104 dominating the geological landscape: (1) the LFS, and (2) the Lattakia Ridge
105 System. The LFS is a sinistral transform fault system linking rifting in the Red Sea
106 with collision in the Taurus (Freund *et al.*, 1970) (fig. 1). Lebanon is located
107 along the LFS on the plate boundary between Africa and Arabia. To the west of
108 the LFS, the area is marked by the stable foreland Levant basin, which was
109 formed synchronously with the Palmyra Basin during the polyphase Mesozoic
110 rifting event (Gardosh *et al.*, 2010).

111

112 Bordering the Levant Basin at its NW boundary is the Lattakia Ridge. This Late
113 Cretaceous structure was established as a result of the subduction of Africa
114 beneath Eurasia starting in the Maastrichtian (Frizon de Lamotte *et al.*, 2011;
115 Stampfli and Hochard, 2009). Continuous compression has marked the region till
116 modern days with an accelerated rollback of the subduction zone along the
117 Hellenic-Cyprus arc during the Tortonian (Le Pichon and Kreamer, 2010) which
118 led to renewed fold-thrust activity in the middle–upper Miocene along the
119 Lattakia Ridge (Hall *et al.*, 2005; Robertson *et al.*, 1996). A regional geodynamic
120 event was witnessed in the Messinian and Pliocene causing a westward tectonic
121 escape of the Anatolian microplate with a component of anticlockwise rotation

122 (Le Pichon and Kreamer, 2010; Sengor and Yilmaz, 1981). It has directly affected
123 the Lattakia Ridge which was reactivated into a sinistral strike-slip motion (Hall
124 *et al.*, 2005). These geodynamic events were marked in both the Levant Basin
125 and onshore Lebanon by reactivation of structures, and a decrease in the lateral
126 motion of the LFS (Freund *et al.*, 1970; Ghalayini *et al.*, 2014; Le Pichon and
127 Gaulier, 1988; Quennell, 1984). It is also at this time, that the accelerated uplift of
128 the pre-existing Lebanese structures took place (Walley, 1998; Ghalayini *et al.*,
129 2017; Beydoun, 1999).

130
131 The thickness of the crust gradually decreases westward from the Palmyrides to
132 the Levant Basin, with 44 km in the SW Palmyrides, 35 km beneath the anti-
133 Lebanon ranges and 27 km beneath Mount Lebanon (Brew *et al.*, 2001; Khair *et*
134 *al.*, 1993). This westward thinning of the crust beneath Syria and Lebanon
135 indicates a transition between a crust of continental type east of the Levant
136 margin, transitioning to a thinned continental crust of 8-10 km thickness
137 beneath the Levant Basin as evidenced by modern gravity inversion (Inati *et al.*,
138 2016) and refraction seismic profiles (Ben-Avraham *et al.*, 2002; Makris *et al.*,
139 1983; Netzeband *et al.*, 2006). This gradual, smooth thickness transition is the
140 result of the Permo-Jurassic rifting of Pangea, causing the break-off of
141 continental blocks from the Afro-Arabian plate to form the Neo-Tethys ocean
142 (Garfunkel, 1998; Robertson, 1998) and pointing to successive regimes of
143 extension that did not reach a real break up stage.

144 **Methods and data**

145

1
2
3
4
5
6
7
8
9
10
11
12
13
14
15
16
17
18
19
20
21
22
23
24
25
26
27
28
29
30
31
32
33
34
35
36
37
38
39
40
41
42
43
44
45
46
47
48
49
50
51
52
53
54
55
56
57
58
59
60

146 Interpretation of three seismic lines along the margin offshore north and south
147 Lebanon were performed (figs 3 to 6). The data used consist of pre-stack depth
148 migrated 3D seismic cube acquired in 2012 by PGS. Streamer length was 7050m
149 long at a spacing of 12.5m and 25m shot point intervals. The interpretation was
150 performed on depth-converted sections. Because no well data were available,
151 time to depth conversion was done using a velocity model built from stacking
152 velocities.

153 **Levant Margin north of Lebanon**

154 **Observations**

155
156 11 horizons were identified in seismic data based on impedance contrast
157 variations and following the interpretation of Hawie *et al.* (2014) (fig. 3). Horizon
158 RN1 separates non-continuous and low amplitude reflectors from the overlying
159 semi-continuous and relatively brighter package. The latter is exhibiting growth
160 strata and fanning geometries. RN2 is a continuous very bright reflector with a
161 strong impedance contrast. Toward the deep basin, it separates a set of bright
162 and stacked continuous reflectors package from non-continuous and dim
163 reflectors. RN3 marks the top of a series of three stacked reflectors package in
164 the east. To the west of the line, it forms an angular unconformity surface in
165 which the underlying unit is truncated. The overlying reflectors also exhibit
166 relatively lower amplitudes. RN4 exhibits a strong impedance contrast and
167 separate chaotic reflectors above from the stacked and bright reflectors below.
168 RN5 is a continuous horizon with a strong impedance contrast marking the top
169 of the low amplitude unit to the east from more continuous and bright reflectors

170 above. It continues westward to the deep basin in which it is still marked by a
171 strong impedance contrast. Horizons RN6 to RN11 were picked up based on the
172 interpretation of Hawie *et al.* (2014).

173

174 The unit between RN2 and RN3 exhibits significant seismic facies variation
175 toward the deep basin in which continuous semi-bright reflectors appear to be
176 transitioning to chaotic reflectors in the middle. Further west, the unit is
177 dominated by a series of stacked and bright reflectors. Similar observations can
178 be made on the unit between RN3 and RN5 to the east in which the reflectors
179 become chaotic in the centre of the line and the overall unit adopts a wedge
180 shape geometry.

181

182 Interpretation

183

184 The fan-shaped geometry of reflectors between RN1 and RN2 point to the
185 presence of growth strata suggesting that normal faults are present at this depth.
186 The latter are NE trending parallel to the coastline and are dipping to the NW.
187 Similar extensional structures are documented in the southern Levant and
188 believed to have nucleated during the Triassic as a result of Tethyan rifting (e.g.
189 Gardosh *et al.* 2010). Therefore, units below RN1 are likely the pre-rift package
190 while units between RN1 and RN2 are the syn-rift package. This could be
191 attributed to the Permian and Triassic-Lower Jurassic units respectively. As RN2
192 is not displaced by faulting and separates deformed units below from non-
193 deformed units above, it could correspond to the break-up unconformity of mid-
194 Jurassic age (Hawie *et al.*, 2014). RN2 therefore marks the initiation of tectonic

1
2
3
4 195 quiescence and gentle subsidence of the Levant region starting the mid to late
5
6 196 Jurassic. The seismic package between RN2 and RN3 likely represents the
7
8 197 Jurassic unit composed of shallow-water, inner to middle shelf carbonates. Its
9
10 198 thickness of 1 – 1.5 km is in coherence with the thickness of the Jurassic in north
11
12 199 Lebanon (Nader *et al.*, 2016; Dubertret, 1955) and is conformable with the
13
14 200 seismic facies interpretation of Hawie *et al.* (2014). Therefore, RN3 could refer to
15
16 201 the Late Jurassic-Early Cretaceous sequence boundary. The seismic facies
17
18 202 transition from continuous to chaotic reflectors indicate mass transport or talus
19
20 203 deposits originating from the Jurassic carbonate platform and deposited at the
21
22 204 distal end of the margin over a slope. The abrupt facies variation into high
23
24 205 amplitude bright reflectors toward the distal basin could point to the presence of
25
26 206 Jurassic clastic units away from the margin.
27
28
29
30
31
32 207
33
34 208 The unit between RN3 and RN4 exhibit a set of stacked high amplitude reflectors
35
36 209 indicating different facies than the adjacent carbonates. They are likely
37
38 210 representing thick bedding which alludes to sand packages of a possibly Lower
39
40 211 Cretaceous age. Therefore, this unit could be analogous to the onshore
41
42 212 Hauterivian Chouf formation, and RN4 could likely represent the top
43
44 213 Hauterivian. The overlying wedge-shape of the unit and the chaotic reflectors
45
46 214 associated could represent mass transport deposits or carbonate talus
47
48 215 originating from the Cretaceous carbonate succession along the margin and
49
50 216 onshore (Hawie *et al.*, 2014). RN5 horizon corresponds to a major marine
51
52 217 onlapping surface and therefore could represent the Senonian unconformity
53
54 218 horizon (Hawie *et al.*, 2014; Gardosh *et al.*, 2011). On top of the Senonian
55
56 219 unconformity, the high amplitude package should be Tertiary in age as it overlies
57
58
59
60

the Cretaceous unit. This unit displays high amplitude reflectors with similar seismic facies to the underlying carbonates unit. Therefore, it could represent Eocene to Miocene carbonate successions. The presence of such Tertiary carbonate units along the Levant margin has been discussed by Hawie *et al.* (2014).

Levant Margin south of Lebanon

Observations

The southern Levant margin offshore Lebanon is marked by a specific structural element termed the Saida-Tyr plateau (STP) which is a 2500 km² elevated Mesozoic plateau as observed in the Senonian unconformity depth map (fig. 4). It is differentiated from the deep Levant basin by large crustal faults to its north and west (figs. 5-6) and is characterized by a thinner Cenozoic unit thickness relative to the remainder of the basin (Hawie *et al.*, 2014).

13 horizons were identified in seismic data based on the interpretation of Hawie *et al.* (2014) and through correlation with the Adloun well, located 5 km east of the seismic line (fig. 5). It was drilled to a depth of 2150 m and reaches the Upper Jurassic unit (Beydoun, 1977). Horizon RS1 separates chaotic non-continuous horizons from a set of semi-continuous thick and bright horizons above. RS2 exhibits a strong impedance contrast separating the overlying chaotic and dim horizons from bright and underlying semi-continuous horizons. It is challenging to assess the continuity of RS1 and RS2 horizons to the west in the deep basin. Horizons RS3 to RS8 are extrapolated from well data and consist of stacked high

1
2
3
4 244 amplitude set of reflectors, with occasional dimming. Horizon RS8 marks the
5
6 245 boundary between stacked high amplitude bright reflectors to the east, and
7
8 246 stacked continuous medium to high amplitude reflectors to the west. The latter
9
10 247 package is pinching out and exhibits onlap on RS8. Horizons RS9 to RS13 are
11
12 248 picked up based on the interpretation of Hawie *et al.* (2014).
13
14
15 249
16
17
18 250 The seismic units between horizon RS2 and RS3, and horizons RS4 and RS5 are
19
20 251 thinning to the west and disappear. Their seismic facies change abruptly from
21
22 252 stacked bright horizons to chaotic. On top of horizon RS2, pinnacle shape
23
24
25 253 buildups are observed. They cover an area of about 200 Km².
26
27
28 254
29
30 255 Large vertical displacement related to vertical faults is observed north and west
31
32 256 of the plateau. The northern bounding fault displaces RS8 horizon 2 km upward
33
34 257 and locally forms a mini-basin along RS12 (fig. 5). The faults to the west have
35
36
37 258 positive-flower geometries with two anticlines observed along their strike (fig.
38
39 259 6). ENE-WSW to ESE-WNW normal faults are observed at the easternmost STP
40
41
42 260 (fig. 5) having a displacement of few hundred meters and extend between RS1
43
44 261 and RS8 horizons. Their strike is ENE-WSW to ESE-WSW.
45
46
47 262
48
49 263 Interpretation
50
51
52 264
53
54 265 From correlation with well data, horizons RS3 to RS7 correspond to Top Jurassic,
55
56 266 Top Hauterivian, Top Aptian, Top Albian and Top Cennomanian. As RS8 horizon
57
58 267 is truncating the Turonian and Senonian units as well as deeper units to the west,
59
60 268 it is believed to be the Senonian unconformity horizon (e.g. Hawie *et al.*, 2013).

1
2
3
4 269 The thickness between RS3 and RS2 is 1.5 to 2 Km, slightly higher than the total
5
6 270 expected thickness of the Jurassic unit south of Lebanon (Nader *et al.*, 2016;
7
8 271 Dubertret, 1955). Horizon RS2 exhibits a strong impedance contrast, probably
9
10 272 indicating a transition between primarily dolomite succession to evaporites.
11
12 273 Therefore, RS2 is likely the top of the mid Triassic. The thickness between RS2
13
14 274 and RS1 is 1 to 1.5 km in accordance with the expected thickness of the Triassic
15
16 275 in Lebanon (Nader *et al.*, 2016; Beydoun and Habib, 1995) and therefore RS1 is
17
18 276 likely the base Triassic. This interpretation points to an extension of the broad
19
20 277 geometries observed onshore to the Levant margin offshore with possible lateral
21
22 278 facies changes expected away from the coast.
23
24
25
26
27
28 279

29
30 280 The interpretation of the Tertiary units is adopted from Hawie *et al.* (2014) in
31
32 281 which horizons RS9 to RS13 correspond to the Eocene Unconformity, Base
33
34 282 Miocene, Base mid Miocene, Base Messinian and Base Pliocene respectively.
35
36 283 These units are overlying the Mesozoic units found eastward and are onlapping
37
38 284 on the Senonian Unconformity horizon, while to east and closer to the shoreline,
39
40 285 the Mesozoic is directly overlain by the Pliocene and the Messinian unit is not
41
42 286 observed in seismic data. This likely indicates an existing topographic high prior
43
44 287 to the deposition of the Tertiary unit. The westward seismic facies variation
45
46 288 observed in the Jurassic and Cretaceous units could be interpreted as talus
47
48 289 deposits originating from the carbonate platform in the East. Overlying the RS2
49
50 290 horizon, the pinnacle shape geometries could consist of local build-ups or
51
52 291 isolated carbonate mounds, though it is challenging to assess their true nature
53
54 292 from seismic data alone.
55
56
57
58
59
60

293

1
2
3
4 294 The large vertical displacement observed on the ENE trending northern
5
6 295 bounding fault, referred to as the Saida fault, is likely related to an old Mesozoic
7
8 296 extensional regime. Ghalayini *et al.* (2014) argues that this fault is reactivated
9
10 297 into a dextral strike-slip in the Late Miocene due to the en-echelon anticlines
11
12 298 observed in the upper Miocene unit. Onshore, the Saida fault is correlated with
13
14 299 the passage of the Damour fault zone, which consists of a deformation zone of
15
16 300 multiple ENE-WSW faults, separating Mount-Lebanon into two different
17
18 301 compartments. It has been suggested that both the Saida and the Damour faults
19
20 302 are the westward continuation of the Jhar fault in Syria due to the similar trend,
21
22 303 evolution history and crustal configuration north and south of these faults
23
24 304 (Ghalayini *et al.*, 2017). Therefore, it is likely that the STP also marks a crustal
25
26 305 transition and could be underlain by a continental crust (e.g. Ghalayini *et al.*,
27
28 306 2014). The western bounding faults displace vertically the Mesozoic unit for
29
30 307 more than 2 km, also suggesting an older extensional episode prior to the
31
32 308 Cenozoic. The positive flower structures and the folding in the Tertiary units
33
34 309 might indicate a transpressive regime starting in the Late Miocene times. The
35
36 310 ENE-WSW to ESE-WNW normal faults documented at the easternmost STP (fig.
37
38 311 5) are similar to faults well documented in southern Mount Lebanon (Homberg
39
40 312 *et al.*, 2009; Homberg *et al.*, 2010). It is very likely that these faults belong to the
41
42 313 same fault family as the ones documented onshore and therefore were active
43
44 314 during the Cretaceous times (e.g. Homberg *et al.* 2009)
45
46
47
48
49
50
51
52
53
54
55

56 315 **Main geological domains**
57
58
59
60 316

317 Based on the available geological data and on the new interpretation of the
318 margin, the Lebanese onshore/offshore area is differentiated into four geological
319 domains, having distinct sedimentological and structural features: (1) the distal,
320 deeper basin, (2) The Lattakia Ridge, (3) the Levant Margin and (3) the onshore
321 (fig. 7). The following sub-sections describe the main geological features of these
322 domains and are as such a review of the available literature. The lithostratigraphic
323 column of the Levant region summarizes the stratigraphy, structures and
324 expected petroleum systems (fig. 8).

325

326 The Deep Basin

327

328 It has formed on an attenuated crust (Inati *et al.*, 2016) during the Triassic and
329 Jurassic when the Neo-Tethys has opened up following the rifting of Pangea. It is
330 characterised by a thick Cenozoic sedimentary cover reaching over 8 km
331 thickness, overlying a Mesozoic succession (Gardosh and Druckman, 2006;
332 Hawie *et al.*, 2013; Roberts and Peace, 2007). The main structural features
333 prevalent in this domain are the normal faults and the NE trending anticlines.

334

335 Stratigraphic setting

336

337 Nine horizons were identified in the Levant basin offshore Lebanon in seismic
338 data and correlated with nearby wells (Hawie *et al.*, 2013). They are believed to
339 correspond to the Mid Jurassic, Jurassic-Cretaceous boundary, Senonian
340 unconformity, Eocene unconformity, Base Miocene, Base mid Miocene, Base

1
2
3
4 341 Messinian and Base Pliocene. The seismic packages are defined by their large-
5
6 342 scale reflection configurations, impedance contrasts, specific stratigraphic
7
8 343 contacts with their lower and upper bounding surfaces, stratal terminations and
9
10 344 overall seismic facies. As the pre-Tertiary units in the deep basin were not drilled
11
12 345 elsewhere in the Levant basin, it is very challenging to separate and seismically
13
14 346 characterize the Mesozoic strata in this domain. The Cenozoic units, such as the
15
16 347 Eocene, Oligocene-Miocene, Messinian and Pliocene, possess higher certainty
17
18 348 and are laterally continuous throughout the Levant basin.
19
20
21 349
22
23
24
25 350 A mixed carbonate-siliciclastic system characterizes the stratigraphy of the deep
26
27 351 basin. The documented units consist of Mesozoic rocks, possibly deep-water
28
29 352 carbonates or clastics, below the Senonian unconformity. The overlying Cenozoic
30
31 353 consists of several units starting with the undercompacted shales of Paleogene
32
33 354 age (Montadert *et al.*, 2014). The Oligo-Miocene units consist of siliciclastic
34
35 355 materials deposited as a result of marginal uplift and sea-level lowstands during
36
37 356 the late Eocene and Oligocene (Haq and Al-qahtani, 2005) which have led to
38
39 357 erosion on the margin and clastic deposition in the basin (Gardosh *et al.*, 2008).
40
41
42 358 Hawie *et al.* (2013) documented the presence of canyons incising the margin
43
44 359 within the middle-upper Miocene offshore northern Lebanon, together with
45
46 360 various characteristics of deep-water sedimentary environments such as
47
48 361 channels, levees and sheeted turbidite lobes towards the distal basin.
49
50
51 362
52
53
54
55
56 363 The thick Oligo-Miocene succession in the Levant Basin can be explained by
57
58 364 considerable sedimentary flux originating from a proto Nile (Steinberg *et al.*,
59
60 365 2011) in which distal turbidites and basin floor fans could extend as far as the

1
2
3
4 366 offshore Lebanon (Dolson *et al.*, 2005; Hawie *et al.*, 2013). However, it was
5
6 367 shown that a multi-source system better describes the filling of the basin based
7
8 368 on forward stratigraphic modelling constrained by seismic, well and field data
9
10
11 369 (Hawie *et al.*, 2015). Therefore, it is most likely that the filling was also
12
13 370 accomplished by erosion from the eastern margin together with provenance of
14
15 371 sediments from the north, mainly from the Lattakia region in Syria. Overlying the
16
17 372 Oligo-Miocene, the Messinian unit is a ~1.7 km thick evaporitic sequence
18
19 373 deposited as a result of the sequestration of the Mediterranean Sea at the end of
20
21 374 the Miocene and contains mass transport complexes at the base, clastic materials
22
23 375 intercalations and halite (Gorini *et al.*, 2015). A return to a pelagic/hemi-pelagic
24
25 376 sedimentation is attested during the Pliocene with the deposition of deep-water
26
27 377 turbidites in the basin (Hawie *et al.*, 2013).
28
29
30
31
32
33
34

35 379 Structural setting

36
37 380
38
39
40 381 NE trending anticlines are documented in the deep basin and are 5 to 15 km long
41
42 382 structures deforming the Oligo-Miocene units only and detaching in the Eocene
43
44 383 unit (fig. 9). Ghalayini *et al.* (2014) argues that these anticlines were folded
45
46 384 immediately prior to, or at the onset of the Messinian salinity crisis due to
47
48 385 absence of growth strata in the pre-Messinian units, and erosion of the anticlinal
49
50 386 crest along the base Messinian horizon. They were formed due to regional
51
52 387 geodynamics caused by the collision and suturing of Arabia with Eurasia. In the
53
54 388 southern Levant, similar trending anticlines were formed and are overlying
55
56 389 deep-seated Mesozoic extensional structures (Gardosh and Druckman, 2006). It
57
58
59
60 390 is not clear if the anticlines offshore Lebanon are overlying deeper reactivated

1
2
3
4 391 structures, but thickness variations below the ones found closer to the margin
5
6 392 strongly suggest so (Ghalayini *et al.*, 2014).
7
8 393
9
10 394 The normal faults are layer bound, found ubiquitously in the Oligo-Miocene units
11
12 395 in the deep basin. The faults are regularly spaced with a dip of 60° either to the
13
14 396 NE or SW. At depth, all the faults consistently die out at the same intra-Eocene
15
16 397 detachment level (fig. 10), which has been interpreted to have a regionally
17
18 398 developed shale sequence acting as the basal detachment surface for these faults
19
20 399 (Montadert *et al.*, 2014; Hawie *et al.*, 2013; Kosi *et al.*, 2012). As there is no NE-
21
22 400 SW extension documented in the basin during the Oligo-Miocene, an exclusive
23
24 401 tectonic origin for their formation or a nucleation model in relation to the
25
26 402 Messinian Salinity Crisis (MSC) has been refuted (Ghalayini *et al.*, 2016). Detailed
27
28 403 analysis of the fault growth and evolution have showed that they have nucleated
29
30 404 during the Early Miocene and remained syn-sedimentary till the Late Miocene
31
32 405 (Ghalayini *et al.*, 2016). A likely nucleation mechanism for these faults could be
33
34 406 related to diagenetic reactions in the Oligo-Miocene units leading to volumetric
35
36 407 contraction of the host rock and causing intra-formational normal faulting (e.g.
37
38 408 Cartwright 2011, Davies *et al.* 2009, Wrona *et al.* 2015).
39
40
41
42
43
44
45
46
47
48
49
50
51
52
53
54
55
56
57
58
59
60

409 **The Lattakia Ridge**

410
411 The Lattakia Ridge is a prominent structure that is found at the NW part of the
412 Levant basin offshore Lebanon. It is part of the Cyprus Arc system and stretches
413 from the Syrian region in the NE to offshore southern Cyprus. It is characterized
414 by a strong topographic high observed at the seafloor.

415

416 Stratigraphic setting

417

418 The stratigraphy in this domain is similar to the rest of the Levant basin, albeit
419 with different thicknesses of units, especially to the west of the ridge itself. The
420 same horizons in the deep basin are also documented along the Lattakia Ridge.
421 The Late Cretaceous convergence has resulted in a depocenter in the lower
422 Tertiary in this region evidenced by thicker Eocene and Oligocene units south
423 and south-east of the Lattakia Ridge (Hawie *et al.*, 2013). The Miocene unit,
424 however, is thinning considerably and reaches up to 1 km in total thickness. It is
425 suggested that the proximity to a northern sedimentary source, i.e. from Syria,
426 could result in coarser sediment and more clastic material in the Oligo-Miocene
427 unit of this domain, possibly pointing to better reservoir qualities (Hawie *et al.*,
428 2015).

429

430

431 Structural setting

432

433 The Latakia Ridge consists of a series of south-east verging thrusts forming
434 prominent NE trending narrow structures and having a profound bathymetric
435 expression (fig. 11). Several anticlines are found adjacent to the Lattakia ridge.
436 These are symmetrical NE-trending structures, which in the Oligo-Miocene units
437 appear very similar to compressional anticlines, while in the deeper Eocene and
438 Mesozoic unit they consist of deep-seated SE verging thrusts with steep SE limbs
439 (fig. 11). Back thrusts are documented along this ridge and are believed to have

1
2
3
4
5
6
7
8
9
10
11
12
13
14
15
16
17
18
19
20
21
22
23
24
25
26
27
28
29
30
31
32
33
34
35
36
37
38
39
40
41
42
43
44
45
46
47
48
49
50
51
52
53
54
55
56
57
58
59
60

440 been initiated during the Pliocene as a result of transpression (Hall *et al.*, 2005;
441 Symeou *et al.*, in review). This complex structural style of the Lattakia Ridge is a
442 result of the geodynamic setting of the Eastern Mediterranean region discussed
443 above.

444 **The Levant margin**

445
446 The Levant margin domain covers the area adjacent to the Lebanese shoreline
447 and comprises the Saida-Tyr plateau, a small narrow strip in front of Beirut, and
448 a larger platform north of Lebanon (fig. 7). It is differentiated from the Cenozoic
449 deeper basin by its thick Mesozoic carbonate succession on top of which the
450 Cenozoic units are pinching out and onlapping. It is generally acknowledged that
451 the Levant margin encompasses the onshore domain in Lebanon, including
452 Mount Lebanon (Nader 2011). However, for the purpose of this paper, we
453 differentiate the Levant margin from the inner onshore domain (i.e. Mount
454 Lebanon and the Bekaa Valley) as the depositional setting and associated
455 petroleum systems are expected to be different (Hawie *et al.*, 2014; Bou Daher *et*
456 *al.*, 2016; Bou Daher *et al.*, 2015; Nader, 2014).

457
458 **Stratigraphic setting**

459
460 Interpretation of the stratigraphy along the Levant margin is provided by Hawie
461 *et al.* (2013), in which they correlate the units identified in seismic data to those
462 documented onshore (Dubertret, 1955; Hawie *et al.*, 2014; Nader, 2011). An

1
2
3
4 463 updated interpretation of the expected stratigraphy of Levant margin is provided
5
6 464 in the previous section of this manuscript.
7
8
9 465

10 11 466 Structural setting 12

13 467
14
15 468 The structures of the southern Levant margin were described in the previous
16
17 469 section. They show an analogy with those described by Ghalayini *et al.* (2014) on
18
19 470 the strike-slip faults, and those of Homberg *et al.* (2009) regarding the normal
20
21 471 faults in southern Lebanon. From south to north, the structural setting of the
22
23 472 Levant margin offshore Lebanon is markedly different. At the latitude of Beirut, a
24
25 473 narrow strip is documented in which the Mesozoic carbonate platform is
26
27 474 considerably narrow or absent. It is correlated with very steeply dipping
28
29 475 Cretaceous strata onshore adjacent to this location (Dubertret, 1955), in contrast
30
31 476 with the broad plateau documented along the southern margin (Homberg *et al.*,
32
33 477 2010; Hancock and Atiya, 1979). In the north, the Tertiary units gently onlap the
34
35 478 Mesozoic succession and the overall margin is cross-cut by E-W trending dextral
36
37 479 strike-slip faults. En-echelon anticlines, oriented NE-SW, are documented in the
38
39 480 Upper Miocene unit along the strike of these strike-slip faults. Several NNE
40
41 481 trending Mesozoic normal faults are documented in the Permo-Triassic units and
42
43 482 could be related to the Mesozoic rifting event (Hawie *et al.*, 2013).
44
45
46
47
48
49
50
51

52 53 483 The onshore domain 54

55 484
56
57 485 The onshore domain comprises the prominent Lebanese ranges including Mount
58
59 486 Lebanon, Anti-Lebanon and the Bekaa Valley in between (fig. 1). It is located at
60

1
2
3
4
5
6
7
8
9
10
11
12
13
14
15
16
17
18
19
20
21
22
23
24
25
26
27
28
29
30
31
32
33
34
35
36
37
38
39
40
41
42
43
44
45
46
47
48
49
50
51
52
53
54
55
56
57
58
59
60

487 the margins of the Levant and the Palmyra Basins, which have similar ages and
488 tectonic histories (Ghalayini *et al.*, 2017; Nader, 2014). Therefore, it has been
489 stated that the Lebanese ranges are part of the Palmyra Basin due to the large
490 resemblance between the structural features, the similar crustal configuration
491 and the analogous stratigraphic intervals (Ghalayini *et al.*, 2017; Beydoun and
492 Habib, 1995; Nader, 2014), yet the Lebanese ranges have been further affected
493 by the passage of the LFS in the Late Miocene and Pliocene. The main folding
494 phase of the Palmyrides and the initial uplift of Mount Lebanon, took place
495 during the Late Oligocene or Early Miocene (Brew *et al.*, 2001; Sawaf *et al.*, 2001;
496 Chaimov *et al.*, 1992; Beydoun, 1999; Hawie *et al.*, 2014; Ghalayini *et al.*, 2017).

497

498 Stratigraphic setting

499

500 The documented units observed in outcrops range from the mid-Jurassic to the
501 Upper Cretaceous in Mount Lebanon, with Paleogene and Neogene sediments
502 closer to the shoreline and in the Bekaa valley. Pre-Jurassic units are not exposed
503 onshore. Nevertheless, correlation with the geology of the Syrian Palmyra basin
504 allowed suggesting that the Triassic sequence is expected to extend westward
505 and is thicker in Lebanon (Beydoun and Habib, 1995). This is based on extensive
506 deep exploration wells and seismic data in Syria (Sawaf *et al.*, 2001; Chaimov *et al.*, 1993; Brew *et al.*, 2001) as well as an old electro-resistivity survey that
507 indicated the presence of a conductive unit located at 650m below the oldest
508 outcropping Jurassic outcrop (Renouard, 1955) which was attributed to a
509 potential Triassic evaporate layer (Beydoun, 1977; Beydoun and Habib, 1995).
511 Therefore, it is likely that the Triassic in Lebanon is analogous to Syria, which has

512 also been proposed based on interpretation of reflection seismic data onshore
513 northern Lebanon (Nader *et al.*, 2016). The Triassic unit in the Palmyrides is
514 documented to consist of a Lower Triassic Amanus shale formation and a middle
515 to Upper Triassic Kurrachine formation. The latter is subdivided into two units, a
516 dolomite and an overlying anhydrite sequence. Equivalent units are identified in
517 Jordan (Luning and Kuss, 2014) and in the southern Levant margin (Gardosh and
518 Tannenbaum, 2014).

519

520 The Jurassic sequence in Lebanon is approximately 1,700 m thick, and could
521 reach 2,700 m thick in the Mount Hermon region of the southern Anti-Lebanon
522 ranges (Dubertret, 1955). The Lower Jurassic consists of a dark and thick
523 dolomite sequence termed the Chouane Dolomites. It is overlain by the mid to
524 late Jurassic Kesrouane Limestone Formation deposited during a period of post-
525 rift subsidence in shallow water environment. Above the Kesrouane formation,
526 lies the Kimmeridgian Bhannes volcanic unit which consists of a mixture of
527 carbonates, marls, lavas and pyroclastics. It is distinctive in some location by its
528 red soils and hard basalts, with occasional pillow lavas. The thickness of this unit
529 decreases southward and is in average around 80-100m thick. Overlying the
530 Bhannes volcanics, is a 60-80 m thick cliff-forming formation termed the Bikfaya
531 formation. It consists of massive bedded limestone deposited in a period of sea
532 level rise. The end of the Jurassic is marked by a return to shallow water
533 sedimentation with deposition of ferruginous oolitic limestone of the Salima
534 formation.

535

1
2
3
4 536 The Cretaceous sedimentary cycle starts with deposition of the Hauterivian
5
6 537 Chouf sandstone formation (Maksoud *et al.*, 2014; Walley, 1997). This unit is
7
8 538 between 5-300 m thick across Lebanon and thins northward reflecting possible
9
10 539 clastic provenance from the southeast. It consists of ferruginous brown to white
11
12 540 sandstone with clays, coaly shales and volcanics. It was deposited under a fluvial
13
14 541 to deltaic littoral environment. The overlying Barremian Abieh formation varies
15
16 542 between fossiliferous limestone, marls and sandstones and represents a
17
18 543 transition between the fluvial Chouf and the overlying shallow marine late
19
20 544 Barremian to Aptian units. The latter is a conspicuous cliff-forming formation
21
22 545 clearly visible throughout all of Lebanon, with a thickness of about 50 m
23
24 546 (Maksoud *et al.*, 2014). It consists of a single massive grey limestone. Small scale
25
26 547 rudist and stromatoporoidal reef buildups are visible in some locations. It
27
28 548 represents a sequence of shallow marine transgressive carbonate facies linked to
29
30 549 early Aptian eustatic rise. The overlying Albian corresponds to thin bedded
31
32 550 carbonates, marls and terrigenous sand. It represents a brief return to
33
34 551 terrigenous clastic deposition, in a general marine setting, before sea levels
35
36 552 caused renewed carbonate deposition.
37
38 553
39
40 554 The upper part of the Cretaceous and early Paleogene is almost entirely
41
42 555 composed of carbonate. The Cennomanian Sannine formation is 600 m thick and
43
44 556 consists of medium to thick bedded shallow water limestones and marly
45
46 557 limestone. This sequence thickens to the west with increasing thin bedded chalk
47
48 558 and cherty pelagic sediments along the coast. It is possible that these lateral
49
50 559 facies change and thickness increase could point to a shift from shallow water
51
52 560 deposition in the east, to deeper environments westward dominated by
53
54
55
56
57
58
59
60

1
2
3
4 561 carbonate turbidite deposits (Hawie *et al.*, 2014). The overlying Turonian unit is
5
6 562 200-300 m thick and represents a continuation of the carbonate deposition of
7
8 563 the Cenomanian and is characterized by thin finely bedded, chalky micrites and
9
10 564 cherts with abundance of Hippurite fossils. The Senonian/Campanian-
11
12 565 Maastrichtian Chekka formation consists of very dark grey to white sequence of
13
14 566 chalks and marly limestone units. Its thickness ranges from 100 to 500 m with
15
16 567 the thickest succession documented in the southern Bekaa valley and is made of
17
18 568 chalk and marly limestone. It has a very good source rock potential as it contains
19
20 569 organic rich argillaceous limestone with TOC values between 2 and 10% (Bou
21
22 570 Daher *et al.*, 2014; Bou Daher *et al.*, 2015).
23
24
25 571
26
27
28
29 572 The overlying Paleocene units are 300 m thick and consist of chalky limestones
30
31 573 and marls. Nummulitic middle Eocene limestone have been documented in the
32
33 574 Bekaa (Dubertret, 1955) where they reach up to 900 m in thickness (Hawie *et al.*,
34
35 575 2014) and in south of Lebanon. The upper Eocene and Oligocene units are absent
36
37 576 in all of Lebanon due to uplift and erosion of the margin during the Early
38
39 577 Miocene compressive folding event (Walley, 1998), except of one outcrop south
40
41 578 of Lebanon (Müller *et al.*, 2010). The middle Miocene is outcropping and consists
42
43 579 of continental lacustrine facies in the Bekaa in contrast with the Miocene open
44
45 580 marine facies along the margin (Hawie *et al.*, 2014; Dubertret, 1955). The
46
47 581 Pliocene in this area is referred to as the Zahle formation (Nader *et al.*, 2016) and
48
49 582 corresponds to clastic deposits, breccias, silt, marl and lacustrine limestone,
50
51 583 overlain by alluvial fan conglomerates (Dubertret, 1955).
52
53 584
54
55
56
57
58
59
60

1
2
3
4 585 Structural setting
5
6 586
7
8
9 587 Mount Lebanon is a NNE trending structure. It exhibits two different structural
10
11 588 styles, similar to the Palmyrides ranges (Brew *et al.*, 2001), separated by a deep
12
13 589 crustal fault that forms the westward extension of the Jhar fault in the
14
15 590 Palmyrides (Ghalayini *et al.*, 2017; Walley, 1998). Northern Mount Lebanon
16
17 591 consists of a broad and symmetric box-fold anticline, (Renouard, 1955; Beydoun
18
19 592 and Habib, 1995), while southern Mount Lebanon is topographically lower and
20
21 593 the deformation zone includes several shorter wavelength folds including a tight
22
23 594 SE verging overfold termed the Niha-Barouk anticline (Dubertret, 1955; Walley,
24
25 595 1998). Anti-Lebanon is an anticlinal structure very similar to Mount Lebanon
26
27 596 located more inland and merges topographically with the Syrian Palmyrides
28
29 597 ranges in the south. The Bekaa valley, which is dominated by a thick Tertiary to
30
31 598 recent continental succession, separates the two mountain ranges. The valley is
32
33 599 narrow in the south in the Hasbaya area and widens northward into the Homs
34
35 600 Plain in Syria.
36
37 601
38
39
40
41
42
43
44 602 The Yammouneh Fault passes through Mount Lebanon and forms a continuation
45
46 603 of the plate boundary between Arabia and Africa that stretches from Aqaba in
47
48 604 the south to Taurus in the North. In Lebanon, it reaches 160 km length and
49
50 605 bounds the eastern side of southern Mount Lebanon, while it cuts through its
51
52 606 northern counterpart. It is believed to be an ancient fault system from pre-
53
54 607 Cambrian times (Butler *et al.*, 1998). The LFS effect in Lebanon is mostly
55
56 608 transpressive resulting in a restraining bend and causing large uplift of the
57
58 609 existing structures during the Pliocene. Since the late Quaternary, it is believed to
59
60

610 accommodate principally strike-slip movements (Daëron *et al.*, 2004; Gomez *et*
611 *al.*, 2006). Transpression and strike-slip tectonics are mainly accommodated by
612 several faults including the Roum and Serghaya Faults. They are major sinistral
613 strike-slip faults branching from the southern LFS in the Golan Heights and
614 accommodate part of the displacement along the LFS (Gomez *et al.*, 2001; Butler
615 *et al.*, 1998).
616
617 Several ENE-WSW, currently active, dextral strike-slip faults are documented
618 along Mount Lebanon (Gedeon, 1999) and extend to the Levant margin offshore
619 (Ghalayini *et al.* 2014). These faults have most likely nucleated during the
620 Mesozoic as normal faults during the breakup of Pangaea and were subsequently
621 reactivated during the Neogene compression (Collin *et al.* 2010; Ghalayini *et al.*
622 2014). Similar faults are also found in the Palmyra basin further east.

623 Petroleum Systems

624 Source rocks and maturity

625
626 Potential source rocks are thought to exist in units between the Permian to
627 Pliocene based on regional stratigraphic correlation, field investigations and
628 geochemical analysis. The major potential source rocks are described here
629 below.

631 The deep basin and Lattakia Ridge

1
2
3
4 633 Geochemical analysis of gas samples from Middle Jurassic to Pliocene reservoirs
5
6 634 along the southeastern margin of the Levant Basin proved the presence of five
7
8 635 thermogenic and biogenic sources (Feinstein *et al.*, 2002). Offshore Lebanon, the
9
10 636 Permian and Triassic thermogenic sources – if present – are believed to generate
11
12 637 petroleum between 90 and 34 Ma in the deep basin (Bou Daher *et al.*, 2016). The
13
14 638 Upper Jurassic Kimmeridgian thermogenic source rocks have most probably
15
16 639 generated oil between the Late Cretaceous and the Late Miocene. The Upper
17
18 640 Cretaceous Campanian might constitute good thermogenic source rocks which
19
20 641 have produced hydrocarbons between 34 and 16 Ma. However, it is expected
21
22 642 that in the deep basin, the Campanian source rock quality and TOC content
23
24 643 would decline (Bou Daher *et al.*, 2015). Paleocene and Eocene thermogenic
25
26 644 source rocks have probably produced hydrocarbons during the Oligocene and
27
28 645 are still active in some parts of the basin.
29
30
31
32
33
34 646
35
36
37 647 The Oligocene unit might constitute potential thermogenic source rocks which
38
39 648 have started to generate hydrocarbons at around 6 Ma and are in the maturity
40
41 649 window at the present day. In addition, the Oligocene is believed to contain a
42
43 650 promising biogenic potential in the deep basin in which generation of biogenic
44
45 651 gas might have occurred between 18.5 and 6 Ma, while on the Lattakia Ridge and
46
47 652 in the more proximal basinal realm it might still be ongoing (Bou Daher *et al.*,
48
49 653 2016) as the units are thinner and located at shallower intervals. In fact, the most
50
51 654 productive biogenic source rocks in the southern Levant are thought to be within
52
53 655 the Oligocene sequence (Gardosh and Tannenbaum, 2014) and these are
54
55 656 expected to extend northward to Lebanon (Hawie *et al.*, 2013; Nader, 2014).
56
57
58
59
60 657 Other biogenic source rocks include the lower and middle Miocene from which

1
2
3
4 658 methane is believed to have been expelled during the Messinian and is currently
5
6 659 ongoing (Bou Daher et al., 2016). Based on thermal history modelling, Bou Daher
7
8 660 *et al* (2016) predicted that a thickness of 700 to 1500m of sub-Messinian
9
10
11 661 Miocene succession is within the biogenic zone at present day. Detailed
12
13 662 information on source rock kinetics, maps of source rock maturation and
14
15 663 transformation ratios are presented in Bou Daher *et al.* (2016).
16
17
18 664

19
20 665 The Levant margin and onshore
21
22
23 666

24
25 667 Permian and Triassic source rocks – if present – would have generated
26
27 668 hydrocarbon between 75 Ma to present day along the margin and onshore (Bou
28
29 669 Daher *et al.*, 2016). In Syria, the upper Permian/Lower Triassic Amanus
30
31 670 dolomites are very good source rocks for Triassic Reservoirs in the Palmyrides
32
33 671 (Barrier *et al.*, 2014) and might therefore be as good in the Levant margin and
34
35 672 onshore. Similarly, the Upper Jurassic Kimmeridgian source rocks most probably
36
37 673 generated oil between the Oligocene to the present day along the margin (Bou
38
39 674 Daher *et al.*, 2016) with minor amount on the onshore in the Late Miocene which
40
41 675 were most probably washed out by meteoric waters (Nader and Swennen,
42
43 676 2004a). However, in the deeply buried Jurassic under the Bekaa Valley, the
44
45 677 Kimmeridgian source rocks are in the oil window today.
46
47
48
49
50

51 678
52
53 679 The Campanian source rocks appears not to have been buried deep enough in
54
55 680 Mount Lebanon to generate hydrocarbon. In the Bekaa valley and along the
56
57 681 margin, however, the Campanian is in the maturity window and minor
58
59 682 generation might have occurred (Bou Daher *et al.*, 2015). Geochemical data
60

1
2
3
4
5
6
7
8
9
10
11
12
13
14
15
16
17
18
19
20
21
22
23
24
25
26
27
28
29
30
31
32
33
34
35
36
37
38
39
40
41
42
43
44
45
46
47
48
49
50
51
52
53
54
55
56
57
58
59
60

683 suggest that the these source rocks are rich in organic sulphur at high TOC (Bou
684 Daher *et al.*, 2014; Bou Daher *et al.*, 2015) leading to hydrocarbon generation at
685 earlier stages of thermal maturity (Bou Daher *et al.* 2016). Large amounts of
686 immature solid bitumen are found in caves and along fault planes in the Bekaa
687 which are typical for early stages of hydrocarbon generation from type IIS
688 kerogen (Bou Daher *et al.*, 2015).

689 **Reservoirs**

690
691 The main reservoirs in the deep basin are found in the Oligo-Miocene unit and
692 consist of sand deposited in deep-water turbidite systems (Gardosh *et al.*, 2008;
693 Hawie *et al.*, 2013). In the lower Miocene unit, the Tamar sand is considered as
694 the best reservoir interval, consisting of sand with high net-to-gross and high
695 porosity/permeability in the range of 20-27% and 500-1000 md respectively
696 (Gardosh and Tannenbaum, 2014). The fact that the Cenozoic unit in the deep
697 basin offshore Lebanon is much thicker than its southern counterpart may
698 suggest that the equivalent potential reservoirs might also be thicker.
699 Investigation of the normal fault system offshore Lebanon has revealed that the
700 growth of faults has been affected by mechanical stratigraphy caused by a strong
701 competent lower Miocene unit with faults nucleating in incompetent fine grained
702 sediments. The competent interval is interpreted to consist of a ~100m thick
703 sandy unit equivalent of the Tamar sand in the south (Ghalayini *et al.*, 2016) or
704 could correspond to another lithology that is mechanically more resistant to
705 faulting.
706

1
2
3
4 707 In the northernmost part of the deep basin and in the Lattakia Ridge domain,
5
6 708 seismic facies interpretation (Hawie *et al.*, 2013) point that the main reservoirs
7
8 709 are possibly located in the upper Miocene and suggest an increased sand content
9
10
11 710 at the base Oligocene. The fact that the normal faults have smaller heights and
12
13 711 displacement in this area point that there is a barrier to vertical fault
14
15 712 propagation (Ghalayini *et al.*, 2014). As the faults do not propagate to the upper
16
17
18 713 Miocene and lower Oligocene units, it is likely that the latter units consist of
19
20 714 incompetent lithologies which might be attributed to coarse clastics or sand. The
21
22 715 provenance of clastic material in this area is most likely from a northerly source,
23
24 716 probably from the Lattakia region in Syria. In addition, the erosion of Cretaceous
25
26 717 to Miocene carbonate platforms contemporaneously with Mount Lebanon's
27
28 718 accelerated uplift in the Late Miocene/Pliocene, could lead to more
29
30 719 conglomeratic material from the northern Lebanese ranges (Hawie *et al.*, 2015;
31
32 720 Hawie *et al.*, 2013).

33
34
35
36
37 721
38
39 722 Along the Levant margin, the Jurassic carbonate platform is far from meteoric
40
41 723 influence prevalent onshore (Nader and Swennen, 2004a). This fact, together
42
43 724 with the predicted presence of fracture-associated hydrothermal dolomites
44
45 725 could form effective reservoirs in the Jurassic carbonate platforms. The Lower
46
47 726 Cretaceous Chouf sandstones are correlated to the Rutbah formation in Syria,
48
49 727 which constitutes the principal reservoir in the Euphrates Graben (Barrier *et al.*,
50
51 728 2014; Sawaf *et al.*, 2001), and to the Helez formation in the southern Levant,
52
53 729 which constitutes the reservoir for the Helez field (Shenhav, 1971). Therefore,
54
55 730 the Chouf sandstone might form good reservoirs in the margin offshore. Other
56
57 731 units in the Cretaceous, such as the Albian and the Aptian, could form good
58
59
60

1
2
3
4 732 reservoirs consisting of isolated reefal buildups similar to the Eratoshtenes
5
6 733 margin (Hawie *et al.*, 2013; Montadert *et al.*, 2014; Esestime *et al.*, 2016).
7
8 734 Younger reservoirs along the Levant margin consist of the lateral ends of the
9
10 735 Oligo-Miocene clastic units onlapping on the Mesozoic carbonate platforms.
11
12 736 These reservoirs are believed to be of good quality due to their proximity to the
13
14 737 Mount Lebanon sedimentary source than their deep basin's equivalent. Miocene
15
16 738 reefs are also documented on paleo-highs along the northern margin and could
17
18 739 provide good reservoirs (Hawie *et al.*, 2013; Hawie *et al.*, 2014).
19
20
21
22 740
23
24
25 741 In the onshore domain below Mount Lebanon, the expected reservoirs are pre-
26
27 742 Jurassic. All exposed units are subject to severe weathering and influx of
28
29 743 meteoric waters, strongly deteriorating the reservoir quality (Nader and
30
31 744 Swennen, 2004a). Good reservoirs could belong to the Permian to lower Triassic
32
33 745 Amanus sand formation consisting of shales interbedded with channel
34
35 746 sandstones and siltstone beds together with the lower to mid Triassic
36
37 747 Kurrachine unit consisting of dolomite and sandy intervals. These units are
38
39 748 important oil and gas reservoirs in the Palmyrides (Barrier *et al.*, 2014) and in
40
41 749 the southern Levant's as they are equivalent to the Mihilla formation (Gardosh
42
43 750 and Tannenbaum, 2014). In the Bekaa region, the reservoirs are believed to be
44
45 751 Jurassic limestones protected from meteoric invasion, Lower Cretaceous
46
47 752 sandstone of the Chouf formation, Upper Cretaceous Senonian fractured
48
49 753 carbonates and Eocene nummulitic limestone.
50
51
52
53
54
55
56
57 754 Seal
58
59
60 755

1
2
3 756 In the deep basin, the Paleocene/Eocene package is believed to form a strong
4
5
6 757 impermeable unit sealing the deeper reservoirs and preventing vertical
7
8 758 hydrocarbon migration from deeper intervals. The consistent detachment of
9
10 759 normal faults on the Eocene unconformity horizon (fig. 10) together with the
11
12 760 chaotic seismic facies and weak amplitudes observed in the Paleocene/Eocene
13
14 761 unit point that the latter is likely constituted by shales (Kosi *et al.*, 2012) and
15
16 762 highly overpressured rocks (Montadert *et al.*, 2014). In the Oligo-Miocene unit,
17
18 763 intra-formational shale or clay may constitute good seals for Miocene reservoirs
19
20 764 similar to the Tamar and other fields in the south (Gardosh *et al.*, 2008). In this
21
22 765 unit, the normal faults could either form good lateral seals at present day or act
23
24 766 as conduits to hydrocarbon migration. In fact, the maximum documented
25
26 767 displacement on these faults is around 350 m, causing a large offset of reservoir
27
28 768 against seal lithologies, increasing the likelihood of impermeability along fault
29
30 769 planes. In contrast, the same faults are observed to cross-cut the Tamar,
31
32 770 Aphrodite and Leviathan fields in the southern Levant basin but they do not
33
34 771 seem to affect the continuity of the reservoirs (Gardosh and Tannenbaum, 2014).
35
36 772 Therefore, this juxtaposition relationship still needs to be checked during
37
38 773 drilling. The shallowest cap rocks in the basin are the Messinian salts forming up
39
40 774 to 1500 m of evaporites and are as such considered to be an optimal seal if
41
42 775 underlying reservoirs are present.
43
44 776
45
46 777 The cap-rocks in the Lattakia Ridge are the same as the ones in the deep basin. In
47
48 778 this area, the complex deformation and extensive fracturation has most probably
49
50 779 affected the sealing potential of all units. This effect is most pronounced at the
51
52 780 Lattakia ridge itself and diminishes south-eastward toward the deep basin. In
53
54
55
56
57
58
59
60

1
2
3
4 781 addition, the Messinian unit is absent on top of the ridge while thinning
5
6 782 considerably in the adjacent areas. Gas chimneys are frequently observed in the
7
8 783 area where the Messinian is absent and/or thinning on top of anticlines SE of the
9
10 784 Lattakia Ridge. In one particular example, gas accumulations in the shallow
11
12 785 upper Miocene reservoirs were possibly leaked out when the seal was thinning
13
14 786 and absent, as evidenced by the chimneys documented only in the absence of the
15
16 787 salt (fig. 12).
17
18
19 788
20
21
22 789 Along the Levant margin, potential cap rocks are the Lower Triassic evaporites of
23
24 790 the Kurrachine formation that are probably extending to the offshore carbonate
25
26 791 platform. The Kimmeridgian volcanic formation might also constitute a good seal
27
28 792 for deeper reservoirs, even though this unit is not laterally homogenous
29
30 793 (Dubertret, 1955) with expected facies change toward the basin. Cretaceous
31
32 794 clays, marls, and basalts could represent good cap rocks for the underlying
33
34 795 reservoirs. The Messinian unit in the Levant margin is either considerably
35
36 796 thinning in some locations (fig. 3) or is absent in others (fig. 5) which could
37
38 797 diminish the Messinian seal quality in this location.
39
40 798
41
42 799 Onshore, the expected thick Upper Triassic evaporites of the Kurrachine
43
44 800 Formation seal the underlying dolomitic reservoirs and protect them from
45
46 801 meteoric influence since the uplift of Mount Lebanon (Nader, 2011). They are
47
48 802 well documented to provide a regional seal in the Palmyrides (Barrier *et al.*,
49
50 803 2014; Sawaf *et al.*, 2001) and in the southern Levant with the equivalent
51
52 804 Saharonim and Mihilla Formations (Gardosh and Tannenbaum, 2014). In the
53
54 805 Bekaa, intra-formational volcanic, marly and shaly units of Jurassic and
55
56
57
58
59
60

806 Cretaceous age could seal the Jurassic and Cretaceous reservoirs. The Paleocene
807 calcareous shales might form a good seal as well as a protection to meteoric
808 infiltration in the Bekaa.

809

810 Traps and migration

811

812 Trap formation in the deep basin offshore Lebanon is mostly related to structural
813 processes in sub-salt units. The structural traps consist of (1) NE trending
814 anticlines in the Oligo-Miocene, detaching on the Eocene unconformity horizon
815 and folded immediately prior to, or at the onset of the Messinian salinity crisis;
816 (2) NE trending transpressive anticlines and positive flower structures found
817 primarily in the south west of the STP and formed during the Late Miocene and
818 (3) Oligo-Miocene tilted fault blocks that nucleated during the lower Miocene
819 and active during Miocene time. Migration of hydrocarbon from biogenic source
820 rocks may have been aided by the intense faulting and fracturing of the Oligo-
821 Miocene unit. As discussed earlier, the faults may constitute a good seal at
822 present day and provide 3-way closures. Their nucleation time during the early
823 Miocene and their continuous activity throughout the Miocene time (Ghalayini *et*
824 *al.*, 2016) make these faults permeable throughout the Miocene. Therefore, any
825 petroleum migration after the Oligocene could result in charging the reservoirs
826 in the Oligo-Miocene unit.

827

828 In the Lattakia Ridge domain, the trap type is mostly structural with symmetrical
829 anticlines in the Cenozoic unit underlain by deep-seated SE verging thrust faults,

1
2
3
4 830 providing excellent four-way closures. These anticlines are found surrounding
5
6 831 the Lattakia Ridge as of the Late Cretaceous time, but the ridge itself is a poor
7
8 832 trap due to the lack of closure as a result of intense uplift and erosion of the
9
10 833 Cenozoic units. Migration of hydrocarbons from source to reservoirs must have
11
12 834 happened through the numerous faults and fractures associated with the intense
13
14 835 deformation of the Lattakia ridge since the Late Cretaceous times. Deformation
15
16 836 continued till modern day indicating that several faults are still active and
17
18 837 implying that they could form effective migration pathways.
19
20
21
22 838
23
24
25 839 Along the Levant Margin, trap mechanism is mostly stratigraphic within the
26
27 840 Mesozoic carbonate platform. Other stratigraphic traps include pinchout of the
28
29 841 Early Cretaceous sand sealed by Cretaceous carbonates in addition to pinchout of
30
31 842 Oligo-Miocene sandy units onto shallower Mesozoic strata and sealed by intra-
32
33 843 Miocene shale. Structural traps include inversion structures, such as reactivated
34
35 844 ENE-WSW strike-slip faults (e.g. Ghalayini et al. 2014) forming 4-way dip
36
37 845 closures below the Messinian. Along the margin, pre-existing and inverted faults
38
39 846 may have played an important role in hydrocarbon migration from the deep
40
41 847 Mesozoic source rocks to shallower reservoirs. As these faults were active
42
43 848 throughout much of the geological time, they might have been permeable during
44
45 849 the Mesozoic and Cenozoic times.
46
47
48
49
50
51 850
52
53
54 851 Onshore, the traps are mostly of structural type, consisting of 4-way dip closure
55
56 852 anticlines formed by the transpression along the LFS (Nader, 2014; Nader *et al.*,
57
58 853 2016). Potential large traps are the Qartaba anticline (Nader, 2014; Nader, 2011)
59
60 854 together with other large structures, such as the Sir-Ed-Denie, Barouk-Niha and

1
2
3
4 855 Jezzine, which might form a good trap geometry in the subsurface similar to the
5
6 856 Qartaba anticline, and could be potential prospects (Beydoun and Habib, 1995;
7
8 857 Beydoun, 1977). They might have formed in the Late Miocene in association with
9
10
11 858 the activity of the LFS. In the Bekaa valley, potential traps might be structures
12
13 859 located beneath the quaternary cover (e.g. Nader *et al.*, 2016).
14
15
16

17 860 Overall Discussion

18
19
20
21 861
22
23 862 Based on 3D seismic data, a new interpretation of the Levant margin offshore
24
25 863 Lebanon is proposed. In the southern margin, the seismic horizons were tied to
26
27 864 nearby well which resulted in updated stratigraphic subdivisions of the Saida-
28
29 865 Tyr plateau. The Triassic unit is likely present based on the predicted unit
30
31 866 thicknesses in Lebanon (Beydoun and Habib, 1995). This is conformable with the
32
33 867 finding of Nader *et al.* (2016) onshore in which they suggest the presence of high
34
35 868 amplitude seismic horizons which they interpret as the Top Triassic based on
36
37 869 regional thicknesses. The high impedance contrasts along this horizon in the
38
39 870 southern margin could be related to the presence of evaporites within the
40
41 871 Triassic but this still needs to be checked by drilling.
42
43
44

45
46
47 872
48
49 873 Recently, the discovery of Zohr in carbonate reservoirs around the Eratosthenes
50
51 874 seamount has opened new play concepts in the basin and attracted attention to
52
53 875 the carbonate potential (e.g. Esestime *et al.*, 2016; Montadert *et al.*, 2014). The
54
55 876 presented interpretation along the margin refines our understanding of the
56
57 877 expected carbonate sequences which could open up new play concepts. The
58
59 878 Mesozoic carbonates are considered to have good porosity from correlation with
60

1
2
3
4 879 onshore analogues in Lebanon (Nader and Swennen, 2004a; Nader and Swennen,
5
6 880 2004b) and Syria (Barrier *et al.*, 2014). As they are sealed from meteoric
7
8 881 invasion, they are very likely not affected by flushing and so are good reservoirs
9
10 882 (e.g. Nader and Swennen 2004a). Hawie *et al.* (2013) demonstrate the presence
11
12 883 of reefal buildups onshore Lebanon based on extensive field observations and
13
14 884 analysis and suggest the likely continuity of such buildups to the margin
15
16 885 offshore. This could make the potential reservoir within the Levant carbonate
17
18 886 sequence equivalent to the Eratosthenes ones and therefore provide effective
19
20 887 analogues for the Zohr (e.g. Esestime et al. 2016). An attractive aspect of the
21
22 888 Levant margin is the strong thermogenic potential in this domain which could
23
24 889 invoke liquid hydrocarbon accumulations.
25
26
27
28
29
30 890
31
32 891 This new interpretation of the margin reduces risk in exploration as it provides
33
34 892 new elements for the petroleum system and hence new potential prospects. The
35
36 893 Lower Cretaceous sandstone is identified in the northern margin,
37
38 894 stratigraphically trapped between the Jurassic and Cretaceous carbonate talus.
39
40 895 This unit offshore appears to be thicker than its equivalent onshore (e.g.
41
42 896 Dubertret, 1955; Bellos, 2008). This could be related to an established
43
44 897 basin/margin differentiation since at least the Early Cretaceous in which a larger
45
46 898 accommodation space is available for the Nubian sand to be deposited offshore.
47
48 899 Hawie *et al.* (2013) indeed argues for a general westward facies variation in
49
50 900 Mesozoic sequences caused by a transition to deeper basinal environments.
51
52
53 901
54
55 902 The relatively good reservoir properties of the Lower Cretaceous sandstone unit
56
57 903 onshore Lebanon and Syria (e.g. Bellos, 2008) and the hydrocarbon production
58
59
60

1
2
3 904 from this same unit in the southern Levant (Shenhav, 1971; Gardosh and
4
5
6 905 Tannenbaum, 2014), suggest that similar prospective plays might well exist
7
8 906 offshore Lebanon. In fact, DHI's such as bright spots and a potential flat-spot is
9
10 907 observed in seismic data (fig. 13) which invoke hydrocarbon accumulations,
11
12 908 originating from thermogenic source rocks. This unit extends along the entire
13
14 909 margin offshore Lebanon and therefore could be associated to large prospects.
15
16
17 910 The challenge, however, is the depth of this play being around 8 km in some
18
19 911 locations, resulting in potentially high pressure reservoirs.
20
21
22
23
24

25 913 Additional DHI's, such as flat spots, can also be observed within the Oligocene
26
27 914 unit along the Levant margin (fig. 14). With the relatively better reservoir quality
28
29 915 expected in this location (Hawie *et al.*, 2015), it is very likely that Oligo-Miocene
30
31 916 pinchout prospects could also be promising. As the flat spot is located below the
32
33 917 Base Miocene horizon, this indicates that the seal might be around the Base
34
35 918 Miocene. This could point that towards the margin, the base Miocene is probably
36
37 919 be associated with shaly/marly or fine grained facies and transitions to coarser
38
39 920 grains or sandy facies toward the basin.
40
41
42
43
44

45 921 **Significance of geological domains**

46
47
48 922

49
50 923 This contribution aims at updating the general knowledge on the potential
51
52 924 petroleum systems of Lebanon ahead to the first Lebanese offshore licensing
53
54 925 round. Based on a comprehensive review of previously published and achieved
55
56 926 integrated research work (geodynamics, stratigraphy, structural geology and
57
58 927 geochemistry) together with the interpretation of two key seismic profiles, we
59
60

1
2
3
4 928 provide here an original subdivision of the Lebanon onshore/offshore into four
5
6 929 distinct geological domains.
7
8 930
9
10
11 931 This subdivision is more adequate when assessing the petroleum potential of
12
13 932 Lebanon as every domain is characterized by a variable petroleum system. This
14
15 933 is due to different geological characteristics of each domain resulting in different
16
17 934 source-reservoir-trap configurations, and hence different petroleum plays.
18
19 935 Therefore, this subdivision becomes very beneficial during exploration as it
20
21 936 focuses attention to specific plays which are a unique to each domain.
22
23
24
25 937
26
27 938 Previous studies have grouped the Lattakia Ridge and the deep basin into one
28
29 939 domain termed the 'offshore' in which a similar petroleum system is expected
30
31 940 (Nader and Swennen, 2004b). More detailed analysis, however, suggests
32
33 941 otherwise. The source rocks charging the reservoirs in the Lattakia Ridge are
34
35 942 supposed to be both thermogenic and biogenic, while in the deep basin the
36
37 943 biogenic ones are dominant (Bou Daher *et al.*, 2016). In addition, the traps are of
38
39 944 Late Cretaceous age and the reservoirs intervals are unlikely to consist of the
40
41 945 Tamar sands but could belong to other intervals (Ghalayini *et al.*, 2014; Ghalayini
42
43 946 *et al.*, 2016; Hawie *et al.*, 2015). Such geological variations necessitate to
44
45 947 associate the Lattakia Ridge to an independent domain of the deep basin.
46
47 948
48
49
50
51
52
53 949 The onshore domain have been discussed abundantly and the expected
54
55 950 petroleum system is well described from regional correlations and field studies
56
57 951 (e.g. Beydoun, 1977; Beydoun and Habib, 1995; Nader and Swennen, 2004b;
58
59 952 Nader, 2014; Hawie *et al.*, 2014). Although the expected source-reservoir
60

1
2
3 953 configurations differ between the Bekaa valley and Mount Lebanon, they have
4
5
6 954 been grouped into one domain. They both are believed to contain a good
7
8 955 thermogenic system (Bou Daher *et al.*, 2016) in which the Triassic petroleum
9
10 956 system is dominant. In the Bekaa, a working Cretaceous petroleum system might
11
12 957 also be effective beneath the quaternary cover (e.g. Nader, 2014; Beydoun,
13
14 958 1977).
15
16
17
18 959

19
20 960 Four petroleum system charts have been compiled for the Lattakia, deep basin,
21
22 961 margin and onshore domains (figs. 15-16). They show the variable petroleum
23
24 962 system elements expected in each. The reservoirs, seals, traps and source rock
25
26 963 maturity have been discussed in previous sections and are summarized in each
27
28 964 chart. In the Lattakia ridge domain and the Levant margin, a mixed
29
30 965 thermogenic/biogenic charge is feeding the reservoirs as of the Late Cretaceous
31
32 966 to modern time, while in the deep basin a dominantly biogenic system is
33
34 967 expected. Onshore, only thermogenic sources are active and charging the
35
36 968 reservoirs as of the late Tertiary.
37
38
39
40
41

42 969 **Regional analogues**

43
44
45 970
46
47
48 971 Comparison between structures and facies documented both offshore and
49
50 972 onshore Lebanon draws similarities between the structural style and reservoirs
51
52 973 of nearby discoveries and therefore decreases uncertainty. Numerous analogue
53
54 974 studies are expected to be carried out in the Levant region in order to bring
55
56 975 further knowledge on such an under-drilled and less known basin. Here, we
57
58
59
60

1
2
3
4 976 provide a few insights on the similarities between onshore and probably similar
5
6 977 offshore structures.
7
8 978
9
10
11 979 The anticlines offshore Beirut (fig. 9) are interpreted to have thin-skinned
12
13 980 deformation in which the Eocene unconformity horizon acts as a detachment
14
15 981 surface (Ghalayini *et al.*, 2014; Kosi *et al.*, 2012). In the southern Palmyrides, the
16
17 982 Triassic salt sequence acts as an effective detachment surface for some of the
18
19 983 anticlines in Syria (Brew *et al.*, 2001). One particular example is the Cheriffe
20
21 984 anticline (Chaimov *et al.*, 1992) which shows a similar structural style to the
22
23 985 offshore Lebanese ones. In addition, some of the anticlines in the Palmyrides
24
25 986 have a box-fold geometry, based on subsurface data and surface expression
26
27 987 (Searle, 1994) drawing analogies to the Qartaba anticline onshore. The latter has
28
29 988 very steep to overturned flanks locally with a gently westward dipping top. This
30
31 989 suggests that the Qartaba anticline is not simply a horst as it was commonly
32
33 990 referred to (Dubertret, 1955) but a compressional structure with possible fault-
34
35 991 propagation folding and/or detachment faulting in which the middle Triassic
36
37 992 evaporates could have acted as a decoupling horizon. In fact, Nader *et al.* (2016)
38
39 993 identified in 2D seismic profiles a deepest horizon in north Lebanon possibly
40
41 994 representing the Triassic evaporites and suggested a continuity of the Qartaba
42
43 995 structure at depth.
44
45 996
46
47 997 Although the effect of the Triassic detachment layer is not observed offshore, the
48
49 998 Eocene unconformity could possess a similar decoupling effect. Therefore, the
50
51 999 thin-skinned anticlines of the Palmyrides are very likely structural analogues for
52
53 1000 the offshore anticlines. In addition, both the offshore and Qartaba anticlines are
54
55
56
57
58
59
60

1001 cross-cut by the same ENE trending dextral strike-slip faults documented along
1002 the Levant margin (Ghalayini *et al.*, 2017). This increases the structural
1003 similarities of these anticlines and insinuates a similar timing, being in the Late
1004 Miocene prior to the effect of the strike-slip faults (e.g. Ghalayini *et al.*, 2014).
1005
1006 The exploration implications on the structural style of the anticlines is profound
1007 as it affects the subsurface closures and location of faults. The uncertainties are
1008 probably less offshore with the availability of 3D seismic data, but the challenges
1009 persist for onshore anticlines. The adopted structural style helps predicting the
1010 likely location of subsurface traps and directly affects the proper positioning of
1011 the wells during exploration. Therefore, using analogues to help exploration
1012 offshore and onshore Lebanon could be of a great value and would reduce
1013 uncertainty significantly.

1014

1015 **Lessons learnt from exploration onshore**

1016

1017 In the onshore domain, exploration wells have been drilled with total depths
1018 ranging from 1,421 m to 3,065 m (Beydoun and Habib, 1995). The deepest
1019 formations reached range in age from Late Cretaceous to mid-Jurassic. In most of
1020 these wells, the main reservoirs were water-flushed due to erosion leading to
1021 bad and ineffective seals, direct communication with elevated meteoric recharge
1022 areas in the high Lebanon and Anti-Lebanon Mountains, or their proximity to
1023 major faults (Nader and Swennen, 2004a; Beydoun and Habib, 1995). Therefore,
1024 it is clear that prospective units must be pre-Jurassic with petroleum system

1
2
3
4 1025 elements similar to the Palmyrides with a probable exception of the Bekaa in
5
6 1026 which the Jurassic and some Cretaceous strata are buried deeper and could be
7
8 1027 well sealed.
9
10 1028
11
12
13 1029 Some of the important lessons acquired for future explorers of the onshore
14
15 1030 Lebanon are the followings: (i) most importantly, the wells must reach the most
16
17
18 1031 promising units, being the Lower Triassic reservoirs that are proven in the
19
20 1032 Palmyrides and (2) analogues must be used to aid exploration – since no
21
22 1033 adequate drilling is available to date. Still hydrocarbon shows were noted in
23
24
25 1034 shallow wells, indicating that a working petroleum system exists. This has also
26
27 1035 been observed offshore with the numerous DHI's, gas chimneys and working
28
29 1036 petroleum system elements, which are all encouraging additional exploration.
30
31
32 1037
33
34 1038 To minimise the risk, it is primordial to use modern techniques to properly
35
36 1039 characterise the prospects and choose the best drilling location. These involve
37
38 1040 (1) reliable seismic data aided by other geophysical data such as gravity,
39
40 1041 magnetic and electrical surveys to image the subsurface at depth, (2) usage of
41
42 1042 satellite imagery and remote sensing to carefully map the structure at surface
43
44 1043 and draw new geological and facies maps over each prospect, and (3) usage of
45
46 1044 new modelling techniques in order to visualise and reconstruct the structure at
47
48 1045 depth. These techniques will substantially reduce the risk of the petroleum
49
50 1046 prospects in the onshore domain. Promising discoveries can be made if new play
51
52 1047 concepts are developed and deeper units are targeted in drilling.
53
54
55
56
57
58
59
60

Conclusions

Interpretations of key seismic reflection profiles along the Levant margin offshore Lebanon together with a comprehensive overview based on recently achieved integrated research projects have resulted in an improved understanding of the geology of this area and of its petroleum exploration potential. Four geological domains have been identified, and petroleum system charts were compiled for each summarizing the main source rocks, reservoirs, seals and traps:

- The deep basin: characterised by predominantly clastic reservoirs and dominated by Oligo-Miocene biogenic source rocks. The structural traps might be late Miocene four-way dip closures and early Miocene tilted fault blocks,
- The Lattakia Ridge: characterised by dominantly Oligo-Miocene clastic reservoirs and with a mixed biogenic-thermogenic source rock potential. The traps are Late Cretaceous four-way dip closures.
- The Levant Margin: characterised by Mesozoic carbonate reservoirs together with Early Cretaceous and Oligo-Miocene clastics, with predominantly thermogenic source rocks with possibility of lateral migration from biogenic source rocks. The traps are mostly stratigraphic.

1
2
3
4 1072 • The onshore: Characterised by Triassic dolomitic, Jurassic and Cretaceous
5
6 1073 carbonate reservoirs with thermogenic source rocks in the Lower
7
8 1074 Triassic, Kimmeridgian and Campanian. The traps are mostly four-way
9
10 1075 dip closures.
11
12
13 1076
14
15 1077 Working petroleum systems are very likely present in Lebanon and should be
16
17
18 1078 encouraging to undertake additional exploration and drilling within these four
19
20 1079 domains. Several lessons can be taken from the wells onshore, which can be used
21
22
23 1080 to better focus future exploration. Nearby discoveries could provide good
24
25 1081 analogue examples for the Lebanese prospects and could help in reducing
26
27 1082 uncertainties, namely onshore. Such analogues are likely found in the
28
29 1083 Palmyrides, and if considered, could positively impact exploration success.
30
31
32
33

34 1084 **Acknowledgements**

35
36
37 1085
38
39
40 1086 The authors are grateful to the Lebanese Petroleum Administration and the
41
42 1087 Ministry of Energy and Water of the Republic of Lebanon for allowing to publish
43
44 1088 the seismic lines in this manuscript and their interpretation. Petroleum Geo-
45
46 1089 services (PGS) are thanked for their support and fruitful discussions. Editor Chris
47
48 1090 Tiratsoo and reviewers [...] are thanked for their constructive reviews and
49
50 1091 comments, which enhanced the quality of this manuscript
51
52
53
54
55

56
57 1092 **References**

58
59
60 1093

- 1094 BARRIER, É., MACHHOUR, L., and BLAIZOT, M., 2014. Petroleum systems of Syria.
 1095 In L. MARLOW, C. KENDALL, and L. YOSE (Eds.), Petroleum systems of the
 1096 Tethyan region, *AAPG Memoir 106*, 335–378.
 1097 <http://doi.org/10.1036/13431862M1063612>
 1098
 1099 BELLOS, G.S., 2008. Sedimentology and diagenesis of some neocomian-
 1100 Barremian rocks (Chouf Formation) southern Lebanon. M.S. thesis, American
 1101 University of Beirut, Beirut, Lebanon.
 1102
 1103 BEN-AVRAHAM, Z., GINZBURG, A., MAKRIS, J., and EPPELBAUM, L., 2002. Crustal
 1104 structure of the Levant Basin, eastern Mediterranean. *Tectonophysics*, **346** (1–2),
 1105 23–43. [http://doi.org/10.1016/S0040-1951\(01\)00226-8](http://doi.org/10.1016/S0040-1951(01)00226-8)
 1106
 1107 BEYDOUN, Z. R., 1977. Petroleum Prospects of Lebanon: Reevaluation. *AAPG*
 1108 *Bulletin*, **61** (I), 43–64. [http://doi.org/10.1306/C1EA3BF4-16C9-11D7-](http://doi.org/10.1306/C1EA3BF4-16C9-11D7-8645000102C1865D)
 1109 [8645000102C1865D](http://doi.org/10.1306/C1EA3BF4-16C9-11D7-8645000102C1865D)
 1110
 1111 BEYDOUN, Z. R., and HABIB, J. G. 1995. Lebanon revisited: new insights into
 1112 Triassic hydrocarbon prospects. *Journal of Petroleum Geology*, **18** (1), 75–90.
 1113
 1114 BEYDOUN, Z.R., 1999. Evolution and development of the Levant (Dead Sea Rift)
 1115 transform system: a historical- chronological review of a structural controversy.
 1116 In: MacNiocaill, C., Ryan, P.D. (Eds.), Continental Tectonics. *Geol. Soc. Lond., Spec.*
 1117 *Publ.*, 164, 239–255 <http://doi.org/10.1144/GSL.SP.1999.164.01.12>
 1118

1
2
3 1119
4
5
6 1120 BOU DAHER, S., DUCROS, M., MICHEL, P., NADER, F. H., and LITTKE, R., 2016. 3D
7
8 1121 thermal history and maturity modelling of the Levant Basin and Margin. *Arabian*
9
10 1122 *Journal of Geosciences*, **17**, 3161. <http://doi.org/10.1007/s12517-016-2455-1>
11
12 1123
13
14
15 1124 BOU DAHER, S., NADER, F. H., MÜLLER, C., and LITTKE, R., 2015. Geochemical
16
17 1125 and petrographic characterization of Campanian – Lower Maastrichtian
18
19 1126 calcareous petroleum source rocks of Hasbayya, South Lebanon. *Marine and*
20
21 1127 *Petroleum Geology*, **64**, 304–323.
22
23 1128 <http://doi.org/10.1016/j.marpetgeo.2015.03.009>
24
25 1129
26
27
28
29 1130 BOU DAHER, S., NADER, F. H., STRAUSS, H., and LITTKE, R., 2014. Depositional
30
31 1131 environment and source-rock characterisation of organic-matter rich Upper
32
33 1132 Santonian-Upper Campanian carbonates, northern Lebanon. *Journal of Petroleum*
34
35 1133 *Geology*, **37**, 5–24.
36
37 1134
38
39 1135 BREW, G. E., BARAZANGI, M., AL-MALEH, A. K., and SAWAF, T., 2001. Tectonic
40
41 1136 and Geologic Evolution of Syria. *GeoArabia*, **6** (4), 573–616.
42
43 1137
44
45 1138 BUTLER, R. W. H., SPENCER, S., and GRIFFITHS, H. M., 1998. The structural
46
47 1139 response to evolving plate kinematics during transpression: evolution of the
48
49 1140 Lebanese restraining bend of the Dead Sea Transform. In Holdsworth, R.E.,
50
51 1141 Strachan, R.A., Dewey, J.F. (Eds.), Continental transpressional and transtensional
52
53 1142 tectonics, *Geol. Soc. Lond., Spec. Publ.* **135**, 81–106.
54
55 1143 [\[doi.org/10.1144/GSL.SP.1998.135.01.06\]](http://doi.org/10.1144/GSL.SP.1998.135.01.06)
56
57
58
59
60

- 1144
- 1145 CARTWRIGHT, J. A., 2011. Diagenetically induced shear failure of fine-grained
- 1146 sediments and the development of polygonal fault systems. *Marine and*
- 1147 *Petroleum Geology*, **28** (9), 1593–1610.
- 1148 (<http://doi.org/10.1016/j.marpetgeo.2011.06.004>)
- 1149
- 1150 CHAIMOV, T. A., BARAZANGI, M., AL-SAAD, D., SAWAF, T., and GEBRAN, A., 1992.
- 1151 Mesozoic and Cenozoic deformation inferred from seismic stratigraphy in the
- 1152 southwestern intracontinental Palmyride fold-thrust belt, Syria. *Geological*
- 1153 *Society of America Bulletin*, **104** (6), 704–715
- 1154 ([doi.org/10.1130/0016-7606\(1992\)104<0704:MACDIF>2.3.CO;2](http://doi.org/10.1130/0016-7606(1992)104<0704:MACDIF>2.3.CO;2))
- 1155
- 1156 CHAIMOV, T. A., BARAZANGI, M., AL-SAAD, D., SAWAF, T., and KHADDOUR, M.
- 1157 (1993). Seismic fabric and 3-D structure of the southwestern intracontinental
- 1158 Palmyride fold belt, Syria. *AAPG Bulletin*, **77** (12), 2032–2047.
- 1159
- 1160 DAËRON, M., BENEDETTI, L., TAPPONNIER, P., SURSOCK, A. and FINKEL, R.C.,
- 1161 2004. Constraints on the post ~25-ka slip rate of the Yammoûneh fault
- 1162 (Lebanon) using in situ cosmogenic ³⁶Cl dating of offset limestone-clast fans:
- 1163 *Earth and Planetary Science Letters*, **227**, 105–119.
- 1164 ([doi:10.1016/j.epsl.2004.07.014](http://doi.org/10.1016/j.epsl.2004.07.014))
- 1165
- 1166 DAVIES, R. J., IRELAND, M. T., and CARTWRIGHT, J. A., 2009. Differential
- 1167 compaction due to the irregular topology of a diagenetic reaction boundary : a
- 1168 new mechanism for the formation of polygonal faults. *Basin Research*, **21**, 354–

1
2
3 1169 359. (doi.org/10.1111/j.1365-2117.2008.00389.x)
4
5
6 1170
7
8 1171 DOLSON, J. C., BOUCHER, P. J., SIOK, J., and HEPPARD, P. D., 2005. Key Challenges
9
10 1172 to realizing full potential in an emerging giant gas province: Nile
11
12 1173 Delta/Mediterranean offshore, deep water, Egypt. In Doré, A. G., Vining, B.A.
13
14 1174 (Eds.), *Petroleum Geology: North-West Europe and Global Perspectives -*
15
16 1175 *Proceedings of the 6th Petroleum geology conference, Petroleum Geology*
17
18 1176 *Conferences*, 607–624. (doi.org/897.553)
19
20 1177
21
22
23
24 1178 DUBERTRET, L., 1955. Carte géologique du Liban au 1/200000 avec notice
25
26 1179 explicative: Beirut, République Libanaise, Ministère des Travaux Publiques, 74
27
28 1180 pp.
29
30 1181
31
32
33 1182 ESESTIME, P., HEWITT, A., and HODGSON, N., 2016. Zohr – A newborn carbonate
34
35 1183 play in the Levantine Basin, East-Mediterranean. *First Break*, **34**, 87–93.
36
37 1184
38
39
40 1185 FEINSTEIN, S., AIZENSHTAT, Z., MILOSLAVSKI, I., GERLING, P., SLAGER, J., and
41
42 1186 MCQUILKEN, J., 2002. Genetic characterization of gas shows in the east
43
44 1187 Mediterranean offshore of southwestern Israel. *Organic Geochemistry*, **33** (12),
45
46 1188 1401–1413. (doi.org/10.1016/S0146-6380(02)00184-5)
47
48 1189
49
50
51
52 1190 FREUND, R., GARFUNKEL, Z., ZAK, I., GOLDBERG, M., WEISSBROD, T., DERIN, B.,
53
54 1191 ... GIRDLER, R. W. (1970). The Shear along the Dead Sea Rift [and Discussion].
55
56 1192 *Philosophical Transactions of the Royal Society A: Mathematical, Physical and*
57
58 1193 *Engineering Sciences*, **267** (1181), 107–130. (doi.org/10.1098/rsta.1970.0027)
59
60

- 1194
- 1195 FRIZON DE LAMOTTE, D., RAULIN, C., MOUCHOT, N., CHRISTOPHE, J., DAVEAU,
1196 W., BLANPIED, C., and RINGENBACH, J. C. (2011). The southernmost margin of
1197 the Tethys realm during the Mesozoic and Cenozoic : Initial geometry and timing
1198 of the inversion processes. *Tectonics*, **30**, 1–22.
1199 (doi.org/10.1029/2010TC002691)
- 1200
- 1201 GARDOSH, M. and DRUCKMAN, Y., 2006. Seismic strati- graphy, structure and
1202 tectonic evolution of the Levantine basin, offshore Israel. In: A.H.F. Robertson
1203 and D. Mountrakis, (Eds.), *Geol. Soc. Lond., Spec. Publ.*, 260, 201 – 227.
- 1204
- 1205 GARDOSH, M., DRUCKMAN, Y., BUCHBINDER, B. and CALVO, R., 2008. The Oligo-
1206 Miocene deepwater system of the Levant Basin. *Geological survey of Israel*, **33**, 1-
1207 73.
- 1208
- 1209 GARDOSH, M. A., GARFUNKEL, Z., DRUCKMAN, Y. and BUCHBINDER, B., 2010.
1210 Tethyan rifting in the Levant Region and its role in Early Mesozoic crustal
1211 evolution. In: Homberg C. and Bachmann M. (Eds), *Evolution of the Levant*
1212 *Margin and Western Arabia Platform since the Mesozoic. Geol. Soc. Lond., Spec.*
1213 *Publ.*, **341**, 9 – 36.
- 1214
- 1215 GARDOSH, M., WEIMER, P., and FLEXER, A., 2011. The sequence stratigraphy of
1216 Mesozoic successions in the Levant margin, southwestern Israel: A model for the
1217 evolution of southern Tethys margins. *AAPG Bulletin*, **95** (10), 1763–1793.
1218 (doi.org/10.1306/02081109135)

1
2
3
4 1219
5
6 1220 GARDOSH, M., and TANNENBAUM, E., 2014. Petroleum systems of Israel. In L.
7
8 1221 MARLOW, C. KENDALL, and L. YOSE (Eds.), Petroleum systems of the Tethyan
9
10 1222 region, *AAPG Memoir 106*, 179–216.
11
12 1223
13
14 1224
15
16
17
18 1225 GARFUNKEL, Z., 1998. Constrains on the origin and history of the Eastern
19
20 1226 Mediterranean basin. *Tectonophysics*, **298** (1–3), 5–35. (doi.org/10.1016/S0040-
21
22 1227 1951(98)00176-0)
23
24
25 1228
26
27
28 1229 GEDEON, M., 1999. Structural analysis of latitudinal faults in the Mount Lebanon
29
30 1230 north of Beirut: their kinematic and their role in the tectonic evolution of
31
32 1231 Lebanon. Master’s thesis, American University of Beirut, Beirut, Lebanon.
33
34 1232
35
36
37 1233 GHALAYINI, R., DANIEL, J.-M., HOMBERG, C., NADER, F. H., and COMSTOCK, J. E.,
38
39 1234 2014. Impact of Cenozoic strike-slip tectonics on the evolution of the northern
40
41 1235 Levant Basin (offshore Lebanon). *Tectonics*, **33** (11), 2121–2142.
42
43 1236 (doi.org/10.1002/2014TC003574)
44
45 1237
46
47
48
49 1238 GHALAYINI, R., HOMBERG, C., DANIEL, J.-M., and NADER, F. H., 2016. Growth of
50
51 1239 layer-bound normal faults under a regional anisotropic stress field. In Childs, c.,
52
53 1240 Holdsworth, R.E., Jackson, C.A.L, Manzocchi, T., Walsh, J.J., Yielding, G. The
54
55 1241 Geometry an Growth of normal faults. *Geol. Soc. Lond., Spec. Publ.* **439**.
56
57 1242 (doi.org/10.1144/SP439.13)
58
59
60 1243

- 1244 GHALAYINI, R., DANIEL, J., HOMBERG, C., NADER, F. H., DARNAULT, R., MENGUS,
1245 J., and BARRIER, E., 2017. The effect of the Palmyra trough and Mesozoic
1246 structures on the Levant margin and on the evolution of the Levant Restraining
1247 bend. In Roure, F., Amin, A., Khomsi, S., Al-Garni, M.A.M. (Eds.), *Lithosphere*
1248 *dynamics and sedimentary basins of the Arabian plate and surrounding areas*,
1249 *Springer*, 149–172. (doi.org/10.1007/978-3-319-44726-1)
1250
1251 GOMEZ, F., KHAWLIE, M., TABET, C., DARKAL, A. N., KHAIR, K., and BARAZANGI,
1252 M., 2006. Late Cenozoic uplift along the northern Dead Sea transform in Lebanon
1253 and Syria. *Earth and Planetary Science Letters*, **241** (3–4), 913–931.
1254 (doi.org/10.1016/j.epsl.2005.10.029)
1255
1256 GOMEZ, F., MEGHRAOUI, M., DARKAL, A. N., SBEINATI, R., DARAWCHEH, R.,
1257 TABET, C., KHAIR, K. and BARAZANGI, M., 2001. Coseismic displacements along
1258 the Serghaya fault: an active branch of the Dead Sea fault system in Syria and
1259 Lebanon. *Journal of the Geological Society*, **158**, 405–408.
1260
1261 GORINI, C., MONTADERT, L., and RABINEAU, M., 2015. New imaging of the
1262 salinity crisis: Dual Messinian lowstand megasequences recorded in the deep
1263 basin of both the eastern and western Mediterranean. *Marine and Petroleum*
1264 *Geology*, 1–17. (doi.org/10.1016/j.marpetgeo.2015.01.009)
1265
1266 HALL, J. T., CALON, T. J., AKSU, A. E., and MEADE, S. R., 2005. Structural evolution
1267 of the Latakia Ridge and Cyprus Basin at the front of the Cyprus Arc , Eastern
1268 Mediterranean Sea. *Marine Geology*, **221**, 261–297.

1
2
3
4 1269 (doi.org/10.1016/j.margeo.2005.03.007)
5
6 1270
7
8 1271 HANCOCK, P. L., and ATIYA, M. S., 1979. Tectonic significance of mesofracture
9
10 1272 systems associated with the Lebanese segment of the Dead Sea transform fault.
11
12 1273 *Journal of Structural Geology*, **1** (2), 143–153. (doi.org/10.1016/0191-
13
14 1274 8141(79)90051-8)
15
16
17 1275
18
19
20 1276 HAQ, B. U., and AL-QAHTANI, A. M., 2005. Phanerozoic cycles of sea-level change
21
22 1277 on the Arabian Platform Rationale for an Arabian Platform Cycle Chart.
23
24 1278 *GeoArabia*, **10** (2), 127–160.
25
26
27 1279
28
29
30 1280 HAWIE, N., GORINI, C., DESCHAMPS, R., NADER, F.H., MONTADERT, L.,
31
32 1281 GRANJEON, D., and BAUDIN, F., 2013. Tectono-stratigraphic evolution of the
33
34 1282 northern Levant Basin (offshore Lebanon). *Mar. Pet. Geo.*, (doi: 10.1016:j.
35
36 1283 marpetgeo.2013.08.004)
37
38
39 1284
40
41
42 1285 HAWIE, N., DESCHAMPS, R., NADER, F.H., GORINI, C., MÜLLER, C., DESMARES, D.,
43
44 1286 HOTEIT, A., GRANJEON, D., MONTADERT, L. and BAUDIN, F., 2014.
45
46 1287 Sedimentologic and stratigraphic evolution of northern Lebanon since the Late
47
48 1288 Cretaceous: implications on the Levant margin and basin. *Arabian Journal of*
49
50 1289 *Geosciences* (DOI: 10.1007/s12517-013-0914-5)
51
52
53 1290
54
55
56 1291 HAWIE, N., DESCHAMPS, R., GRANJEON, D., NADER, F.H., GORINI, C., MULLER, C.,
57
58 1292 MONTADERT, L. and BAUDIN, F., 2015. Multi-scale constraints of sediment
59
60 1293 source to sink systems in frontier basins: a forward stratigraphic modeling case

- 1294 study of the Levant region. *Basin Research* 1–28, doi: 10.1111/bre.12156
- 1295
- 1296 HOMBERG, C., BARRIER, É., MROUEH, M., HAMDAN, W., and HIGAZI, F., 2009.
- 1297 Basin tectonics during the Early Cretaceous in the Levant margin, Lebanon.
- 1298 *Journal of Geodynamics*, **47** (4), 218–223. (doi.org/10.1016/j.jog.2008.09.002)
- 1299
- 1300 HOMBERG, C., BARRIER, É., MROUEH, M., MÜLLER, C., HAMDAN, W., and HIGAZI,
- 1301 F., 2010. Tectonic evolution of the central Levant domain (Lebanon) since
- 1302 Mesozoic time. In Homberg, C. and Bachmann, M. (Eds.), Evolution of the Levant
- 1303 margin and western Arabia platform since the Mesozoic, *Geol. Soc. Lond., Spec.*
- 1304 *Publ.*, **341**, 245–268. (doi.org/10.1144/SP341.12)
- 1305
- 1306 INATI, L., ZEYEN, H., NADER, F. H., ADELINET, M., SURSOCK, A., ELIE, M., and
- 1307 ROURE, F., 2016. Lithospheric architecture of the Levant Basin (Eastern
- 1308 Mediterranean region): A 2D modeling approach. *Tectonophysics*, **693**, 143–156.
- 1309 (doi.org/10.1016/j.tecto.2016.10.030)
- 1310
- 1311 KHAIR, K., KHAWLIE, M., HADDAD, F., BARAZANGI, M., SEBER, D., and CHAIMOV,
- 1312 T. A., 1993. Bouguer gravity and crustal structure of the Dead Sea transform fault
- 1313 and adjacent mountain belts in Lebanon. *Geology*, **21**, 739–742.
- 1314
- 1315 KOSI, W., TARI, G., NADER, F. H., SKIPPLE, C., TRUDGILL, B. D., and LAZAR, D.,
- 1316 2012. Structural analogy between the “piano key faults” of deep-water Lebanon
- 1317 and the extensional faults of the Canyonlands grabens, Utah, United States. *The*
- 1318 *Leading Edge*, (July), 824–830.

1
2
3 1319
4
5
6 1320 LE PICHON, X., and GAULIER, J. M., 1988. The rotation of Arabia and the Levant
7
8 1321 fault system. *Tectonophysics*, **153** (1–4), 271–294. (doi.org/10.1016/0040-
9
10 1322 1951(88)90020-0)
11
12 1323
13
14
15 1324 LE PICHON, X., and KREAMER, C., 2010. The Miocene-to-Present Kinematic
16
17 1325 Evolution of the Eastern Mediterranean and Middle East and Its Implications for
18
19 1326 Dynamics. *Annual Review of Earth and Planetary Science*, **38**, 323–351.
20
21 1327 (doi.org/10.1146/annurev-earth-040809-152419)
22
23 1328
24
25
26
27 1329 LUNING, S., and KUSS, J., 2014. Petroleum Geology of Jordan. In L. MARLOW, C.
28
29 1330 KENDALL, and L. YOSE (Eds.), Petroleum systems of the Tethyan region, *AAPG*
30
31 1331 *Memoir 106*, 149-172.
32
33 1332
34
35
36
37 1333 MAKRIS, J., BEN-AVRAHAM, Z., BEHLE, A., GINZBURG, A., GIESE, P., STEINMETZ,
38
39 1334 L., ... ELEFTHERIOU, S., 1983. Seismic refraction profiles between Cyprus and
40
41 1335 Israel and their interpretation. *Geophysical Journal International*, **75**, 575–591.
42
43 1336
44
45
46
47 1337 MAKSOUD, S., RANIER, B.G., AZAR, D., GEZE, R., PAICHELER, J.P. and MORENO-
48
49 1338 BEDMAR, J., 2014. Revision of ‘ Falaise de B LANCHE ’ (Lower Cretaceous) in
50
51 1339 Lebanon , with the definition of a Jezzinian Regional Stage: *Carnets de Geologie*,
52
53 1340 **14**, 401–427.
54
55 1341
56
57
58 1342 MONTADERT, L., NICOLAIDES, S., SEMB, P. H., and LIE, O. (2014). Petroleum
59
60 1343 Systems offshore Cyprus. In L. MARLOW, C. KENDALL, and L. YOSE (Eds.),

- 1
2
3 1344 Petroleum systems of the Tethyan region, *AAPG Memoir 106*, 301–334.
4
5
6 1345 MONTADERT, L., SEMB, P. H., LIE, O., and KASSINIS, S., 2010. New seismic may
7
8 1346 put offshore Cyprus hydrocarbon prospects in the spotlight. *First Break*, **28**
9
10 1347 (April), 91–101.
11
12 1348
13
14
15 1349 MÜLLER, C., HIGAZI, F., HAMDAN, W., and MROUEH, M., 2010. Revised
16
17 1350 stratigraphy of the Upper Cretaceous and Cenozoic series of Lebanon based on
18
19 1351 nannofossils. In Homberg, C. and Bachmann, M. (Eds.), Evolution of the Levant
20
21 1352 margin and western Arabia platform since the Mesozoic, *Geol. Soc. Lond., Spec.*
22
23 1353 *Publ.*, **341**, 287–303. (doi.org/10.1144/SP341.14)
24
25 1354
26
27
28
29 1355 NADER, F. H., and SWENNEN, R., 2004a. Petroleum prospects of Lebanon: some
30
31 1356 remarks from sedimentological and diagenetic studies of Jurassic carbonates.
32
33 1357 *Marine and Petroleum Geology*, **21** (4), 427–441. (doi.org/10.1016/S0264-
34
35 1358 8172(03)00095-3)
36
37
38 1359
39
40
41 1360 NADER, F. H., and SWENNEN, R., 2004b. The hydrocarbon potential of Lebanon:
42
43 1361 new insights from regional correlations and studies of Jurassic dolimitization.
44
45 1362 *Journal of Petroleum Geology*, **27** (3), 253–275.
46
47 1363
48
49
50
51 1364 NADER, F. H., 2011. The petroleum prospectivity of Lebanon: an overview.
52
53 1365 *Journal of Petroleum Geology*, **34**, 135–156.
54
55 1366
56
57
58 1367 NADER, F. H., 2014. Insights into the petroleum prospectivity of Lebanon. In L.
59
60 1368 MARLOW, C. KENDALL, and L. YOSE (Eds.), Petroleum systems of the Tethyan

1
2
3
4 1369 region, *AAPG Memoir 106*, 241–278. (doi.org/10.1036/13431859M1063609)
5
6 1370
7
8 1371 NADER, F. H., BROWNING-STAMP, P., and LECOMTE, J. C., 2016. Geological
9
10 1372 intepretation of 2D seismic reflection profiles onshore Lebanon: implications for
11
12 1373 petroleum exploration. *Journal of Petroleum Geology*, **39**, 333–356.
13
14 1374
15
16
17 1375 NETZEBAND, G., GOHL, K., HÜBSCHER, C., BEN-AVRAHAM, Z., DEHGHANI, G. A.,
18
19 1376 GAJEWSKI, D., and LIERSCH, P., 2006. The Levantine Basin—crustal structure
20
21 1377 and origin. *Tectonophysics*, **418** (3–4), 167–188.
22
23 1378 (doi.org/10.1016/j.tecto.2006.01.001)
24
25 1379
26
27
28 1380 QUENNELL, A. M., 1984. The Western Arabia rift system. In R. J. Dixon, R.J.,
29
30 1381 Robertson, A.H.F. (Eds.), *The geological evolution of the Eastern Mediterranean*,
31
32 1382 *Geol. Soc. Lond., Spec. Publ.*, **17**, 775–788.
33
34 1383 (doi.org/10.1144/GSL.SP.1984.017.01.62)
35
36 1384
37
38
39 1385 RENOUARD, G., 1955. Oil prospects of Lebanon. *AAPG Bulletin*, **39** (11), 2125–
40
41 1386 2169.
42
43 1387
44
45
46 1388 ROBERTS, G., and PEACE, D., 2007. Hydrocarbon plays and prospectivity of the
47
48 1389 Levantine Basin , offshore Lebanon and Syria from modern seismic data.
49
50 1390 *GeoArabia*, **12** (3).
51
52
53 1391
54
55
56 1392 ROBERTSON, A. H. F., 1998. Tectonic significance of the Eratosthenes Seamount:
57
58 1393 a continental fragment in the process of collision with a subduction zone in the
59
60

- 1394 eastern Mediterranean (Ocean Drilling Program Leg 160). *Tectonophysics*, **298**
1395 (1–3), 63–82. (doi.org/10.1016/S0040-1951(98)00178-4)
1396
1397 ROBERTSON, A. H. F., DIXON, J. E., BROWN, S., COLLINS, A., MORRIS, A. P.,
1398 PICKETT, E., ... USTAOMER, T., 1996. Alternative tectonic models for the Late
1399 Palaeozoic-Early Tertiary development of Tethys in the Eastern Mediterranean
1400 region. In Morris, A., Tarling, D.H. (Eds.), *Palaeomagnetism and tectonics of the*
1401 *Mediterranean region. Geol. Soc. Lond., Spec. Publ.*, **105**, 239–263.
1402 (doi.org/10.1144/GSL.SP.1996.105.01.22)
1403
1404 SAWAF, T., BREW, G. E., LITAK, R. K., and BARAZANGI, M., 2001. Geologic
1405 evolution of the intraplate palmyride basin and euphrates fault system syria. In
1406 P. A. Ziegler, P.A, Cavazza, W., Robertson, A.H.F., Crasquin-Soleau, S. (Eds.), *Peri-*
1407 *Tethys Memoir 6: Peri-Tethyan rift/Wrench basins and passive margins,*
1408 *Memoire du Museum national d’histoire naturelle, Paris*, 441–467).
1409 SEARLE, M.P., 1994. Structure of the intraplate eastern Palmyride fold belt, Syria:
1410 *Geological Society of America Bulletin*, **106**, 1332–1350. (doi: 10.1130/0016-
1411 7606(1994)106<1332)
1412
1413 SENGOR, A. M. C., and YILMAZ, Y., 1981. Tethyan evolution of Turkey: a plate
1414 tectonic approach. *Tectonophysics*, **75**, 181–241.
1415
1416 SHENHAV, H., 1971. Lower Cretaceous Sandstone Reservoirs, Israel:
1417 Petrography, Porosity, Permeability. *AAPG Bulletin*, **55** (12), 2194–2224.
1418 (doi.org/10.1306/819A3E30-16C5-11D7-8645000102C1865D)

1
2
3 1419
4
5
6 1420 STAMPFLI, G. M., and HOCHARD, C., 2009. Plate tectonics of the Alpine realm. In
7
8 1421 Murphy, J.B., Keppie, J.D., Hynes, A.J. (Eds.), Ancient orogens and modern
9
10 1422 analogues, *Geol. Soc. Lond., Spec. Publ.* **327**, 89–111(doi.org/10.1144/SP327.6)
11
12 1423
13
14
15 1424 STEINBERG, J., GVIRTZMAN, Z., FOLKMAN, Y., and GARFUNKEL, Z., 2011. Origin
16
17 1425 and nature of the rapid late Tertiary filling of the Levant Basin. *Geology*, **39** (4),
18
19 1426 355–358. (doi.org/10.1130/G31615.1)
20
21
22 1427
23
24
25 1428 SYMEOU, V., HOMBERG, C., NADER, F.H., DARNAULT, R., LECOMTE, J.C. &
26
27 1429 PAPADIMITRIOU, N. *In review*. Longitudinal and temporal evolution of the
28
29 1430 tectonic style along the Cyprus Arc system, assessed through 2D reflection
30
31 1431 seismic interpretation.
32
33 1432
34
35
36 1433 WALLEY, C.D., 1997. The lithostratigraphy of Lebanon: a Review. Lebanese
37
38 1434 Scientific Bulletin, 10, 81-108
39
40
41 1435
42
43
44 1436 WALLEY, C.D., 1998. Some outstanding issues in the geology of Lebanon and
45
46 1437 their importance in the tectonic evolution of the Levantine region.
47
48 1438 Tectonophysics, 298, 37-62.
49
50
51 1439
52
53
54 1440 WETZEL, R., 1974. Etapes de la prospection petroliere en Syrie et au Liban
55
56 1441 (Notes et mémoires). *Compagnie Francaise des Petroles*, Paris.
57
58 1442
59
60 1443 WRONA, T., JACKSON, C. A., HUUSE, M., and TAYLOR, K. G., 2015. Silica diagenesis

1444 in Cenozoic mudstones of the NorthViking Graben : physical properties and basin
1445 modelling. *Basin Research*, 1–20. (doi.org/10.1111/bre.12168)

1446

1447

1448 Figures

1449

1450 Fig1: Main structural elements of Lebanon, the Levant Basin and part of Syria. Map
1451 compiled from Barrier et al. 2014; Ghalayini et al. 2016; Ghalayini et al. 2014; Brew
1452 et al. 2001.

1453

1454 fig. 2: Creaming curve for both the Oligo-Miocene 4-way dip closures and the
1455 Mesozoic carbonate plays in the Levant Basin.

1456

1457 Fig. 3: Geo-seismic line showing the Levant margin off the coast of northern Lebanon
1458 consisting mainly of a carbonate succession. The Triassic contains extensional
1459 normal faults in relation to the Triassic breakup of Pangea and the Early Cretaceous
1460 clastics are pinching out on the Jurassic carbonate talus deposits.

1461

1462 Fig. 4: Structural map of the Saida-Tyr plateau offshore and the onshore Tyr-
1463 Nabatieh plateau. The depth map offshore corresponds to the Senonian
1464 unconformity horizon. The en-echelon anticlines along the Saida fault are only
1465 observed at the Base Messinian horizon and not at the level of the Senonian
1466 unconformity.

1467

1468 Fig. 5: Geo-seismic line showing the Levant margin off the coast of southern

1
2
3 1469 Lebanon. The broad Mesozoic platform in this area is referred to as the Saida-Tyr
4
5 1470 Plateau (Ghalayini et al. 2014). The seismic data was tied to the nearby Adloun well
6
7
8 1471 and shows the complete Jurassic to Cretaceous succession found onshore. The
9
10 1472 strong reflectors below the Jurassic are believed to represent the Triassic. For
11
12 1473 location, see figure 4.
13
14 1474
15
16
17 1475 Fig. 6: Geoseismic line across the western edge of the Saida-Tyr plateau showing
18
19 1476 the transgressive anticlines separating the deep basin from the Mesozoic plateau.
20
21 1477 For location, see figure 4.
22
23
24 1478
25
26 1479 Fig 7: The geological domains of Lebanon together with the nearby hydrocarbon
27
28 1480 discoveries
29
30
31 1481
32
33 1482 Fig. 8: Petroleum potential, stratigraphy and tectonic events for Lebanon and its
34
35 1483 offshore
36
37
38 1484
39
40 1485 Fig. 9: An example of a NE trending anticline in the deep basin domain offshore
41
42 1486 Lebanon. The structural style suggests detachment folding on an intra-Eocene
43
44 1487 horizon. The anticlines were folded in the Late Miocene prior to the Messinian event
45
46 1488 (Ghalayini *et al.* 2014).
47
48
49 1489
50
51 1490 Fig 10: Seismic section showing the titled fault blocks in the deep basin domain. The
52
53 1491 depth map of the base mid Miocene horizon shows the geometry of the associated
54
55
56 1492 traps at present day
57
58 1493
59
60 1494 Fig. 11: Geo-seismic line showing the Latakia Ridge north of the Levant Basin

1
2
3 1495
4

5
6 1496 Fig. 12: gas chimneys on top of a Miocene anticline observed only when the

7
8 1497 Messinian seal thins or is absent. The overlying Pliocene exhibits numerous bright

9
10 1498 spots and DHI's pointing to entrapment of the leaked gas into Pliocene reservoirs in

11
12 1499 structural closures.
13

14
15 1500
16

17 1501 Fig. 13: Geoseismic line showing a bright spot and a potential flat spot in the Lower

18
19 1502 Cretaceous unit pinching out along the Levant margin and trapped between

20
21 1503 Mesozoic carbonates.
22

23
24 1504
25

26 1505 Fig. 14: Geoseismic line showing a potential flat spot in the Oligocene unit observed

27
28 1506 along the Levant margin. The lateral Oligo-Miocene units are pinching out on the

29
30 1507 margin forming classical stratigraphic traps.
31

32
33 1508
34

35 1509 Fig. 15: Petroleum system charts for the deep basin and Latakia Ridge domains.

36
37 1510
38

39
40 1511 Fig. 16: Petroleum system charts for the Levant margin and onshore domains.
41
42
43
44
45
46
47
48
49
50
51
52
53
54
55
56
57
58
59
60

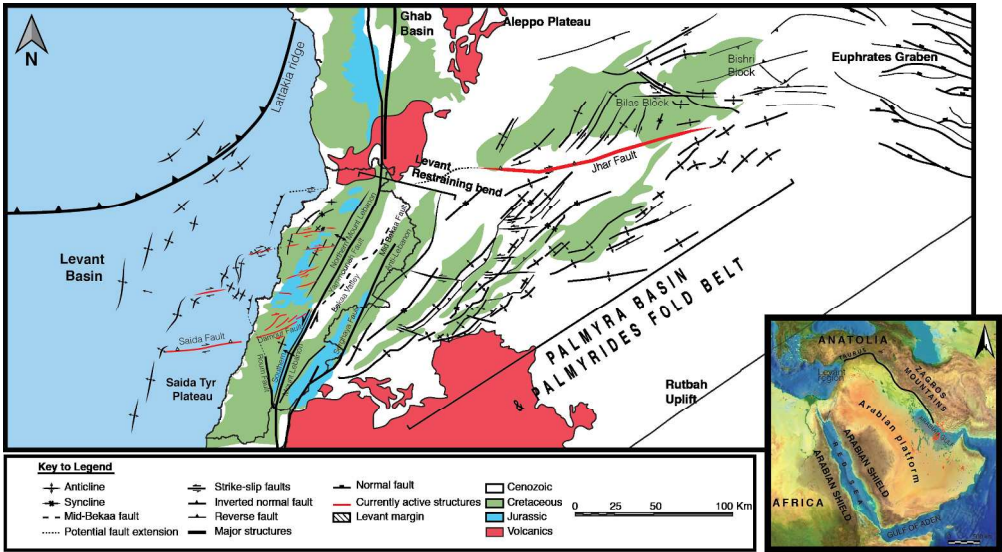


Figure 1

Main structural elements of Lebanon, the Levant Basin and part of Syria. Map compiled from Barrier et al. 2014; Ghalayini et al. 2016; Ghalayini et al. 2014; Brew et al. 2001.

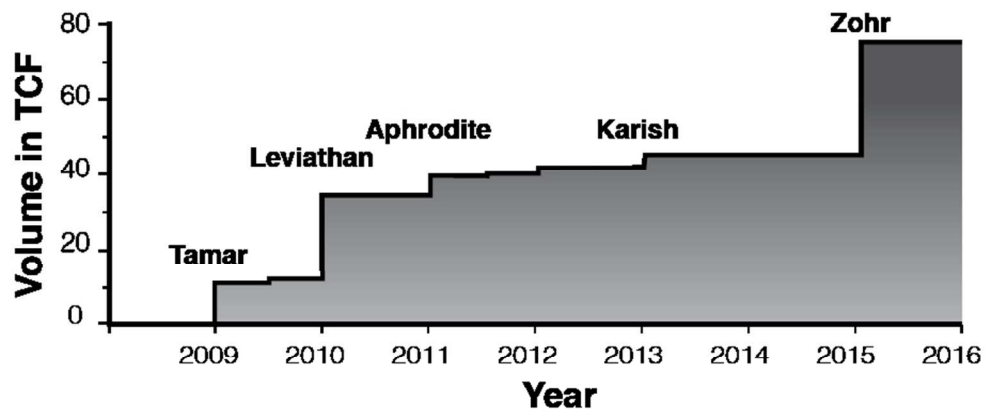


Figure 2

Creeping curve for both the Oligo-Miocene 4-way dip closures and the Mesozoic carbonate plays in the Levant Basin.

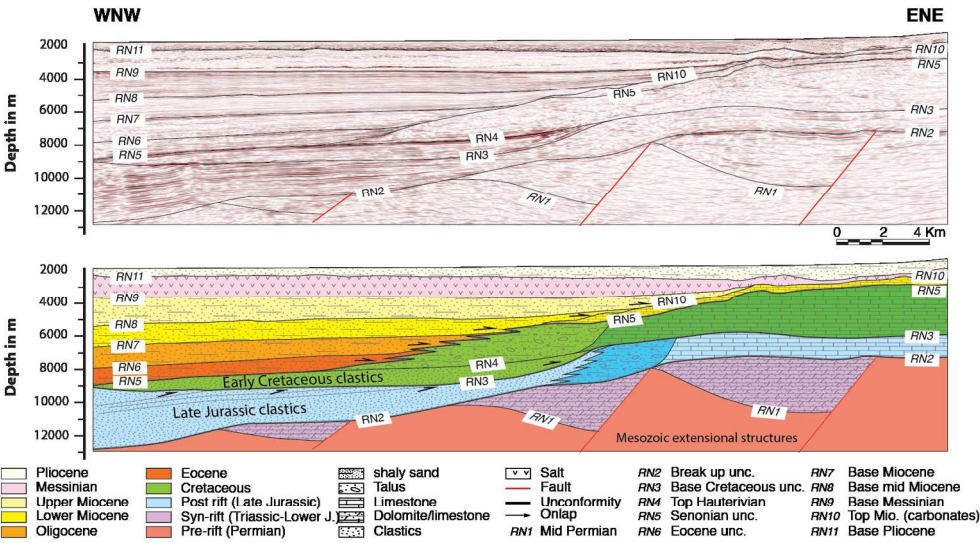


Figure 3

Geo-seismic line showing the Levant margin off the coast of northern Lebanon consisting mainly of a carbonate succession. The Triassic contains extensional normal faults in relation to the Triassic breakup of Pangea and the Early Cretaceous clastics are pinching out on the Jurassic carbonate talus deposits.

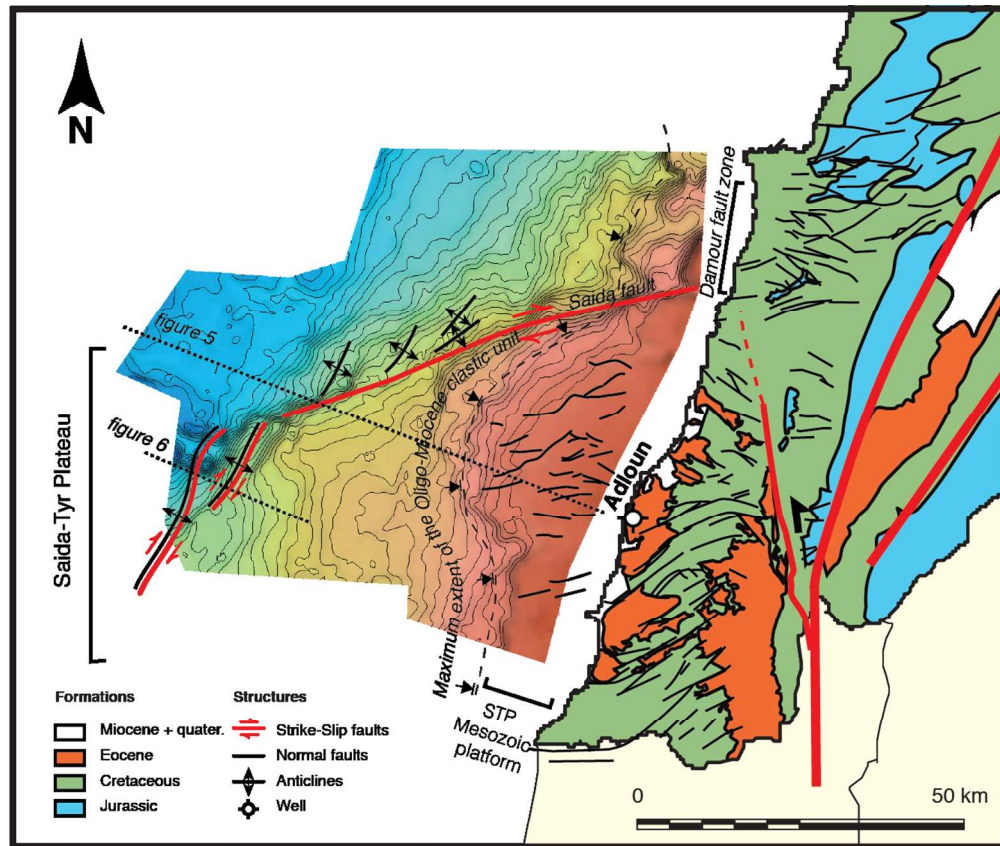


Figure 4

Structural map of the Saida-Tyr plateau offshore and the onshore Tyr-Nabatieh plateau. The depth map offshore corresponds to the Senonian unconformity horizon. The en-echelon anticlines along the Saida fault are only observed at the Base Messinian horizon and not at the level of the Senonian unconformity.

1
2
3
4
5
6
7
8
9
10
11
12
13
14
15
16
17
18
19
20
21
22
23
24
25
26
27
28
29
30
31
32
33
34
35
36
37
38
39
40
41
42
43
44
45
46
47
48
49
50
51
52
53
54
55
56
57
58
59
60

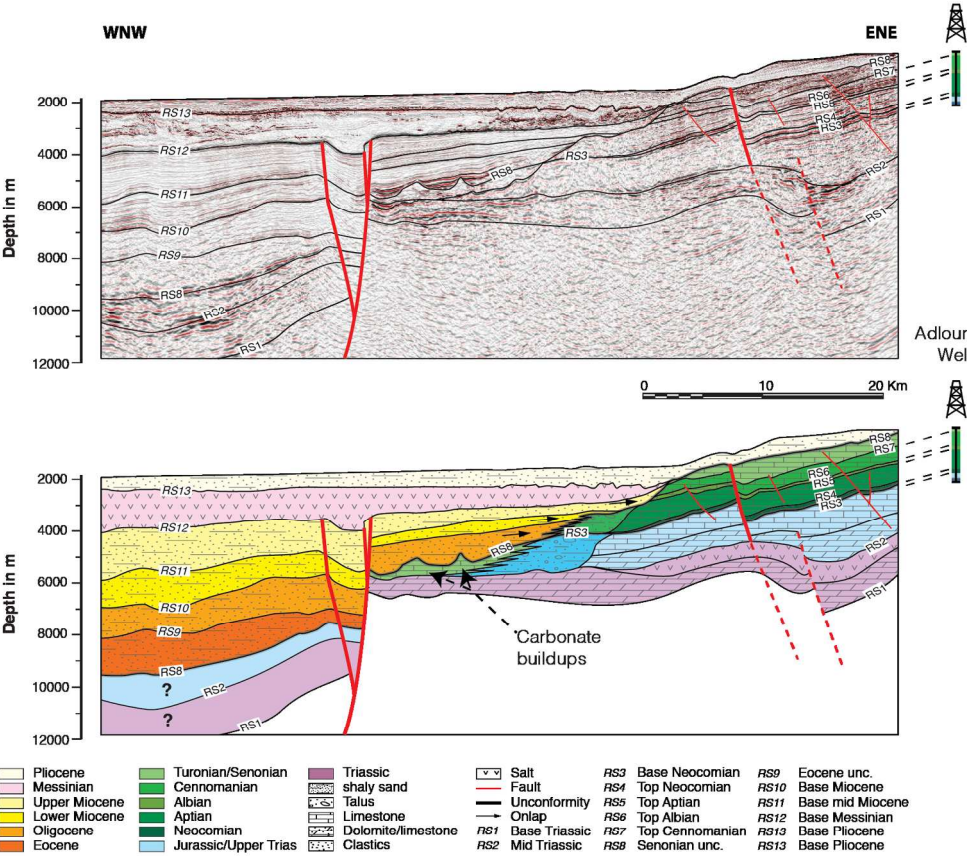
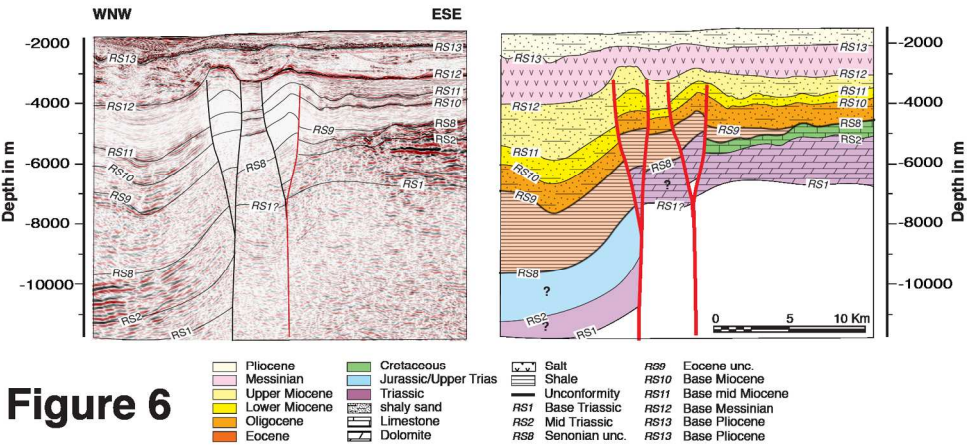
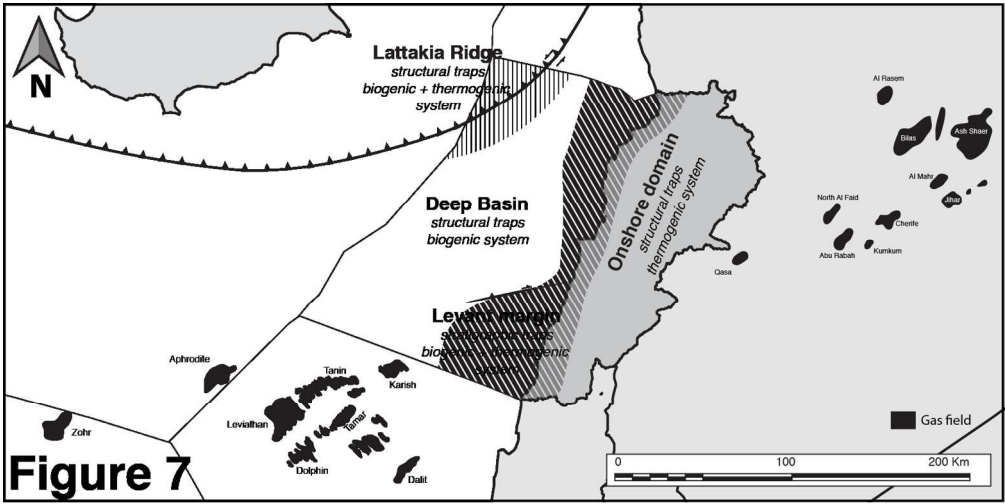


Figure 5

Geo-seismic line showing the Levant margin off the coast of southern Lebanon. The broad Mesozoic platform in this area is referred to as the Saida-Tyr Plateau (Ghalayini et al. 2014). The seismic data was tied to the nearby Adloun well and shows the complete Jurassic to Cretaceous succession found onshore. The strong reflectors below the Jurassic are believed to represent the Triassic. For location, see figure 4.



Geoseismic line across the western edge of the Saida-Tyr plateau showing the transgressive anticlines separating the deep basin from the Mesozoic plateau. For location, see figure 4.



The geological domains of Lebanon together with the nearby hydrocarbon discoveries.

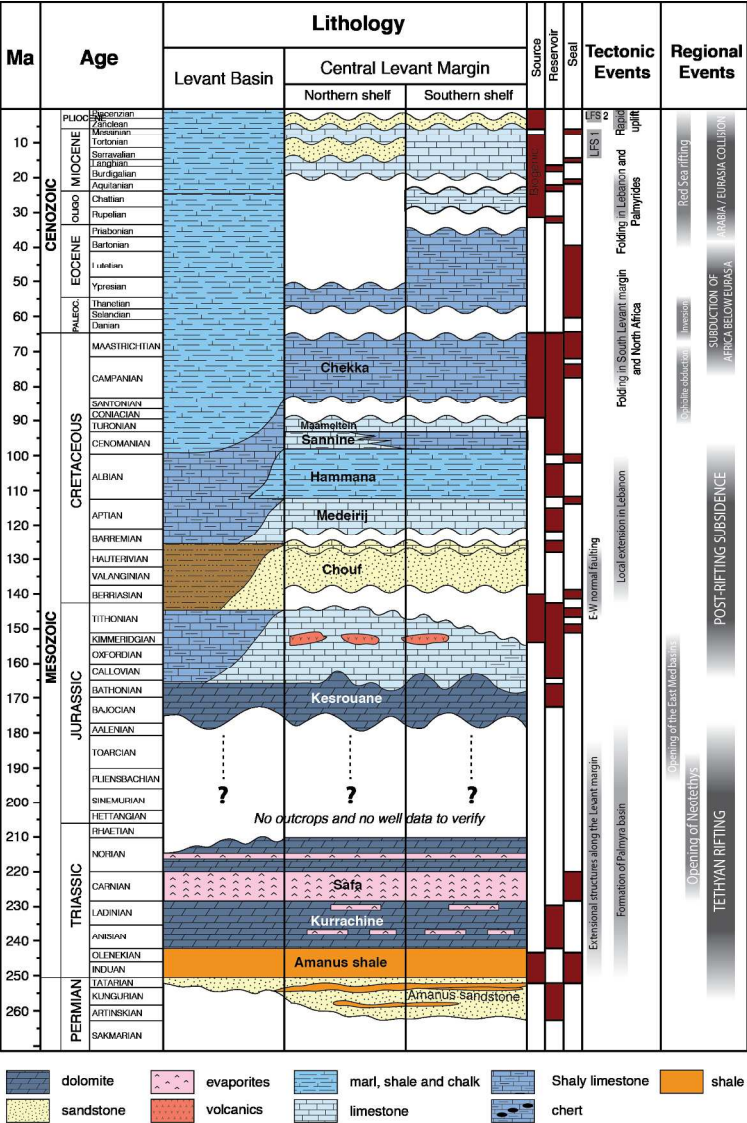


Figure 8

Petroleum potential, stratigraphy and tectonic events for Lebanon and its offshore.

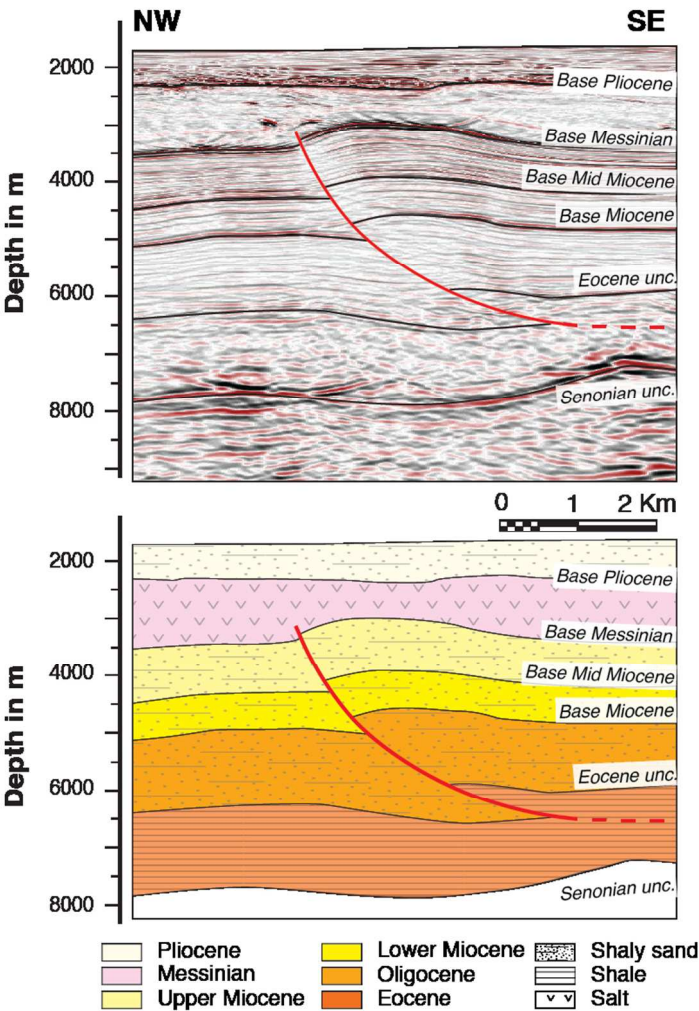


Figure 9

An example of a NE trending anticline in the deep basin domain offshore Lebanon. The structural style suggests detachment folding on an intra-Eocene horizon. The anticlines were folded in the Late Miocene prior to the Messinian event (Ghalayini et al. 2014).

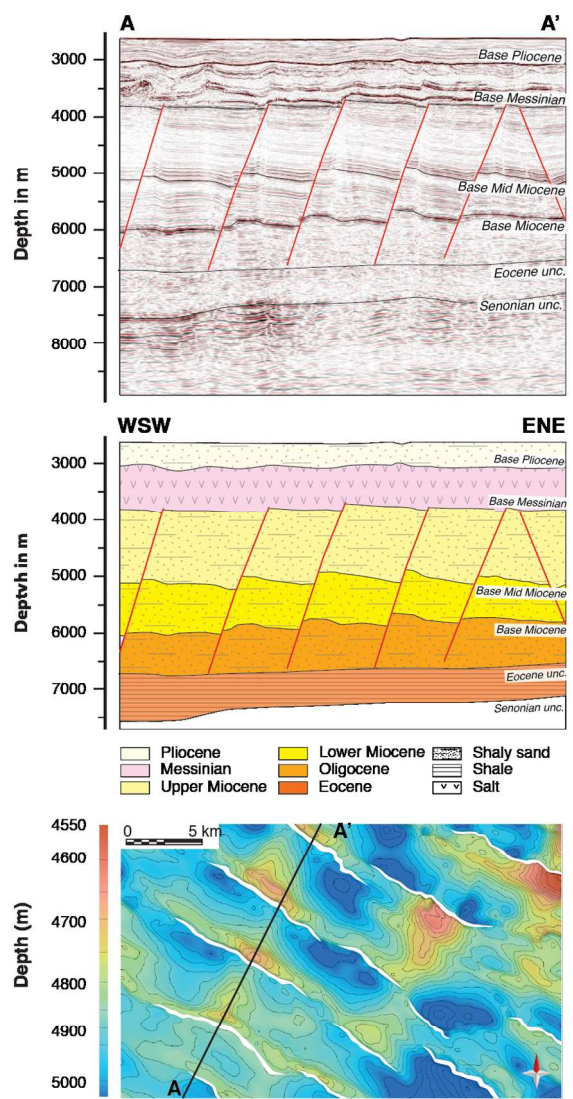


Figure 10

Seismic section showing the titled fault blocks in the deep basin domain. The depth map of the base mid Miocene horizon shows the geometry of the associated traps at present day.

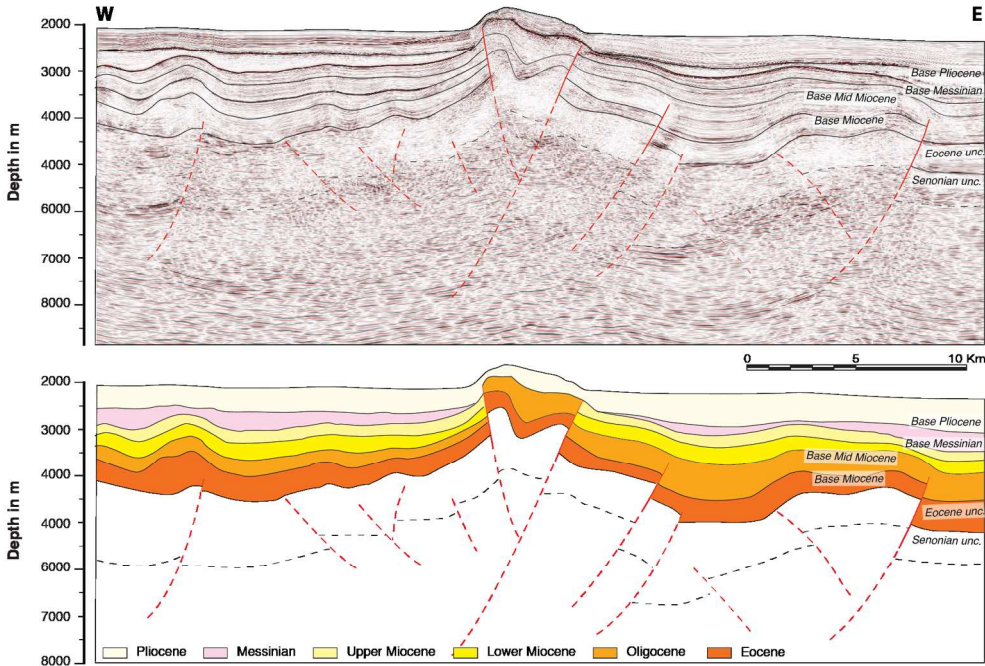


Figure 11

Geo-seismic line showing the Latakia Ridge north of the Levant Basin

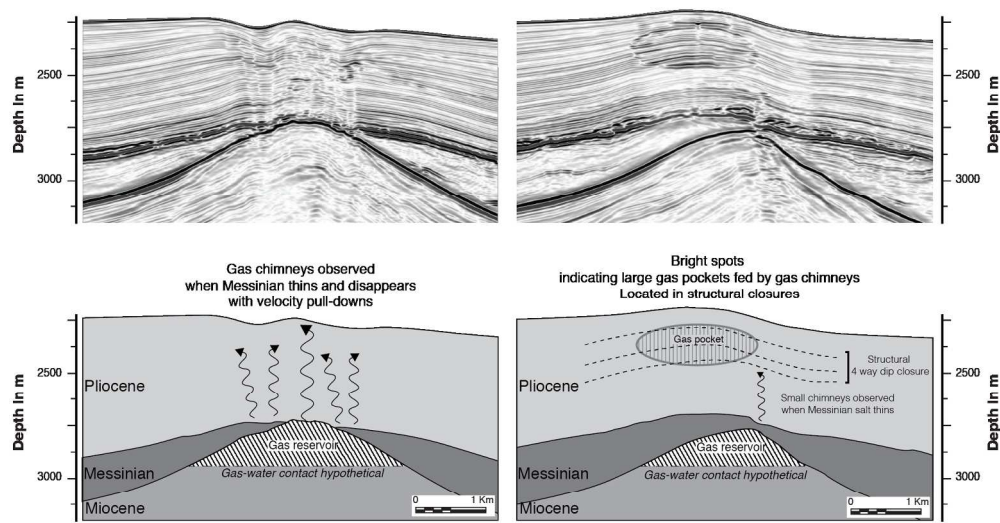


Figure 12

gas chimneys on top of a Miocene anticline observed only when the Messinian seal thins or is absent. The overlying Pliocene exhibits numerous bright spots and DHI's pointing to entrapment of the leaked gas into Pliocene reservoirs in structural closures.

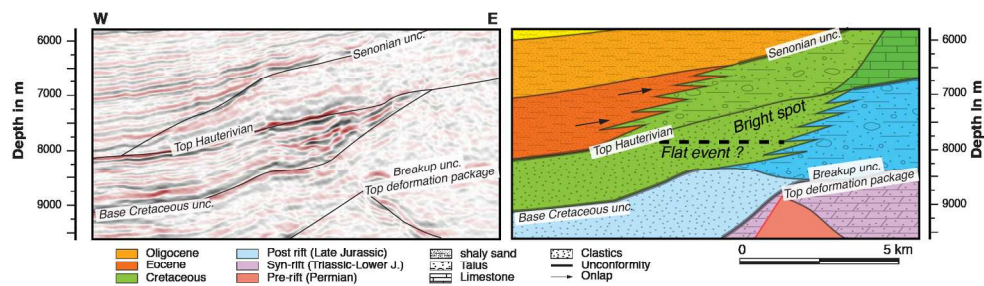


Figure 13

Geoseismic line showing a bright spot and a potential flat spot in the Lower Cretaceous unit pinching out along the Levant margin and trapped between Mesozoic carbonates.

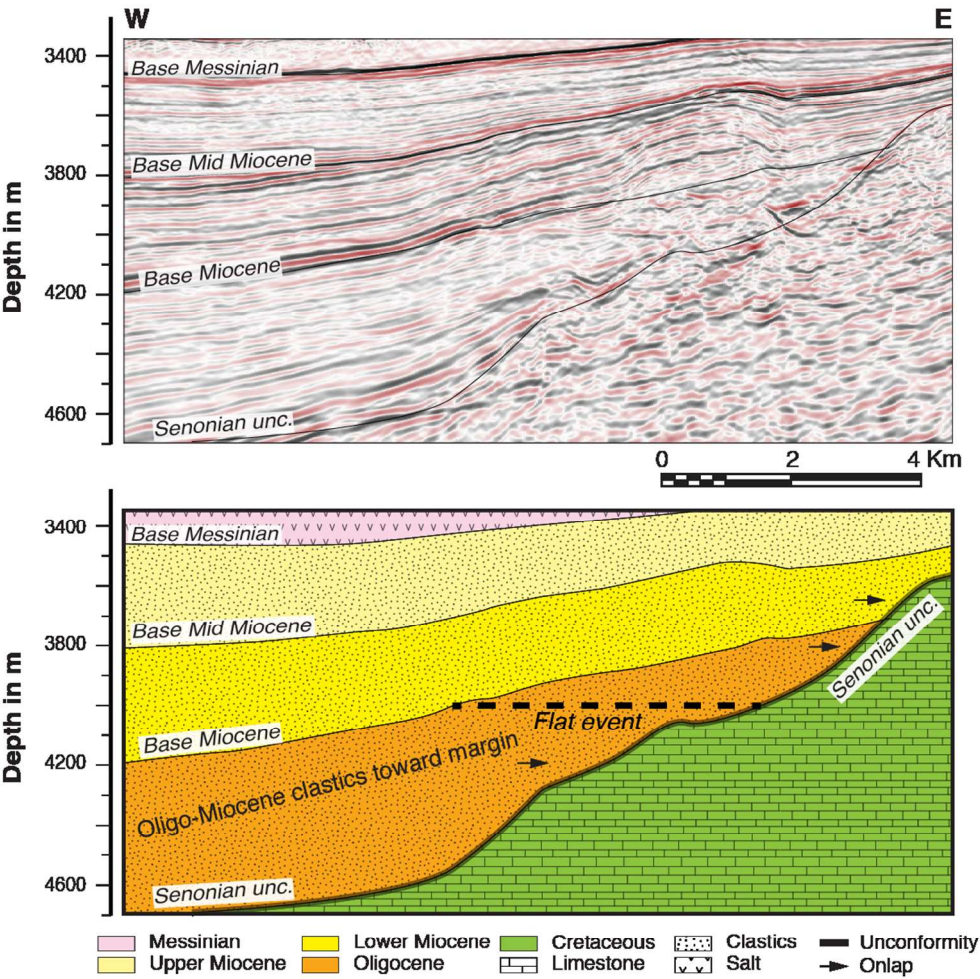


Figure 14

Geoseismic line showing a potential flat spot in the Oligocene unit observed along the Levant margin. The lateral Oligo-Miocene units are pinching out on the margin forming classical stratigraphic traps.

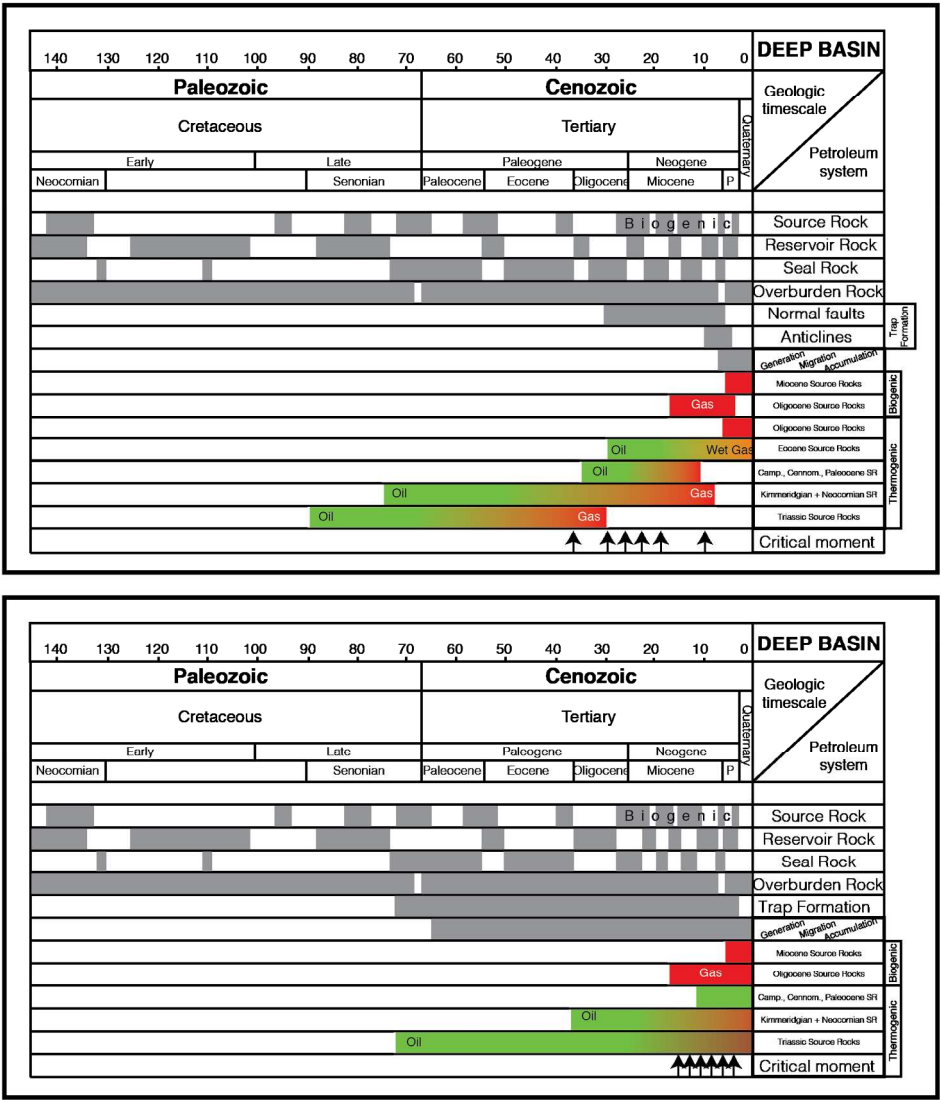


Figure 15

Petroleum system charts for the deep basin and Latakia Ridge domains.

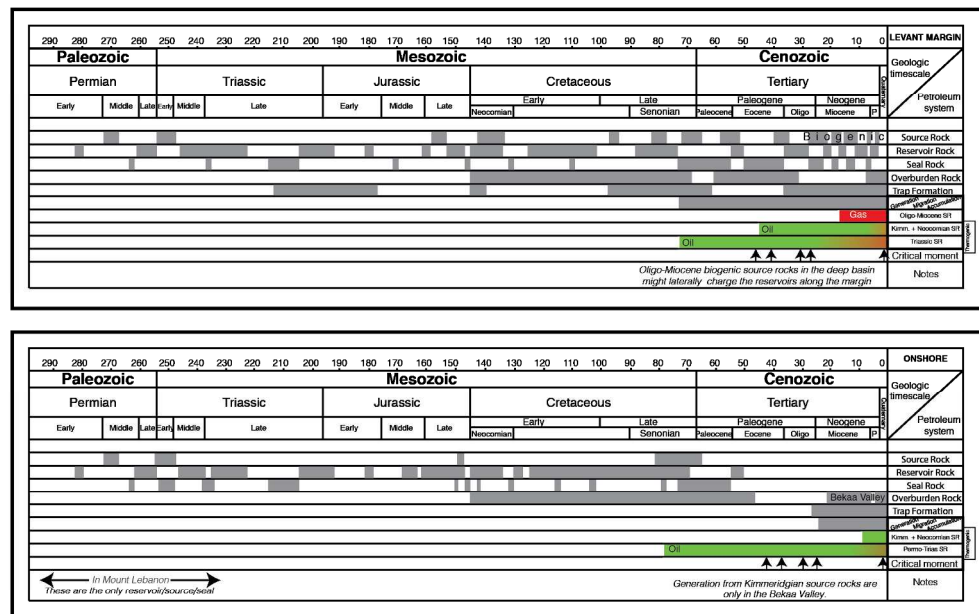


Figure 16

Petroleum system charts for the Levant margin and onshore domains.